

Journal Pre-proof

From Methylene Bridged Diindole to Carbonyl Linked Benzimidazoleindole:
Development of Potent and Metabolically Stable PCSK9 Modulators

Haibo Xie, Ka Yang, Gabrielle N. Winston-McPherson, Donnie S. Stapleton, Mark P. Keller, Alan D. Attie, Kerry A. Smith, Weiping Tang



PII: S0223-5234(20)30650-4

DOI: <https://doi.org/10.1016/j.ejmech.2020.112678>

Reference: EJMECH 112678

To appear in: *European Journal of Medicinal Chemistry*

Received Date: 13 June 2020

Revised Date: 16 July 2020

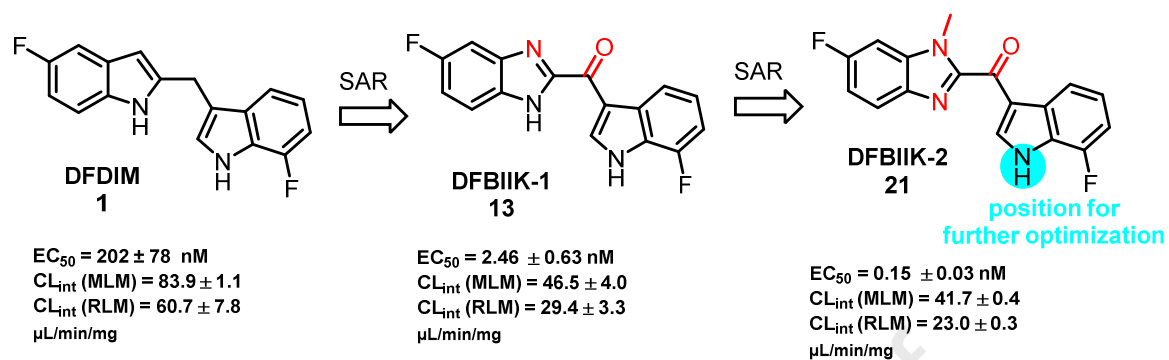
Accepted Date: 18 July 2020

Please cite this article as: H. Xie, K. Yang, G.N. Winston-McPherson, D.S. Stapleton, M.P. Keller, A.D. Attie, K.A. Smith, W. Tang, From Methylene Bridged Diindole to Carbonyl Linked Benzimidazoleindole: Development of Potent and Metabolically Stable PCSK9 Modulators, *European Journal of Medicinal Chemistry*, <https://doi.org/10.1016/j.ejmech.2020.112678>.

This is a PDF file of an article that has undergone enhancements after acceptance, such as the addition of a cover page and metadata, and formatting for readability, but it is not yet the definitive version of record. This version will undergo additional copyediting, typesetting and review before it is published in its final form, but we are providing this version to give early visibility of the article. Please note that, during the production process, errors may be discovered which could affect the content, and all legal disclaimers that apply to the journal pertain.

© 2020 Elsevier Masson SAS. All rights reserved.

Graphical Abstract



Highlights

- Novel PCSK9 modulators were synthesized and evaluated in cell-based assays.
- Compound **21** can potently reduce PCSK9 protein in cell-based assays.
- Compound **21** has improved metabolic stability.
- Compound **21** could be a potential candidate for the treatment of hyperlipidemia.

Journal Pre-proof

From Methylene Bridged Diindole to Carbonyl Linked Benzimidazoleindole: Development of Potent and Metabolically Stable PCSK9 Modulators

Haibo Xie,^{1‡} Ka Yang^{1‡} Gabrielle N. Winston-McPherson,¹ Donnie S. Stapleton,² Mark P. Keller,² Alan D. Attie,² Kerry A. Smith,¹ and Weiping Tang^{1,3*}

¹ School of Pharmacy, University of Wisconsin-Madison, Madison, Wisconsin 53705, United States

² Department of Biochemistry, University of Wisconsin-Madison, Madison, Wisconsin 53706, United States

³ Department of Chemistry, University of Wisconsin-Madison, Madison, Wisconsin 53706, United States

*Corresponding author: School of Pharmacy, University of Wisconsin-Madison, Madison, WI 53705,

USA. E-mail: weiping.tang@wisc.edu (Weiping Tang)

‡These authors (H. X. and K. Y.) contributed equally.

Keywords

PCSK9, Phenotypic screening, Fluorine scan, Metabolic stability, Indole

Abstract

Proprotein convertase subtilisin/kexin type 9 (PCSK9) is a recently validated therapeutic target for lowering low-density lipoprotein cholesterol (LDL-C). Through phenotypic screening, we previously discovered a class of small-molecules with a 2,3'-**diindolymethane** (DIM) skeleton that can decrease the expression of PCSK9. But these compounds have low potency and low metabolically stability. After performing structure-activity relationship (SAR) optimization by nitrogen scan, deuterium substitution and fluorine scan, we identified a series of much more potent and metabolically stable PCSK9 modulators. A preliminary *in vivo* pharmacokinetic study was performed for representative analogues

difluorodiindolyketone (DFDIK) 12 and **difluorobenzoimidazolylindolyketone (DFBIK-1) 13**. The *in vitro* metabolic stability correlate well with the *in vivo* data. The most potent compound **21** has the EC₅₀ of 0.15 nM. Our SAR studies also indicated that the NH on the indole ring of **21** can tolerate more function groups, which may facilitate the mechanism of action studies and also allow further improvement of the pharmacological properties.

Introduction

Cardiovascular diseases (CVD) is the number one cause of death world-wide. High levels of low-density lipoprotein (LDL), clinically known as hypercholesterolemia or hyperlipidemia, are strongly associated with CVD. Although statin therapy has been very successful for many patients, about 20% of them are not able to achieve target LDL levels due to the adverse effects of statin therapy. Proprotein convertase subtilisin/kexin type 9 (PCSK9) is secreted from the liver, binds to the LDL receptor (LDLR), and causes its lysosomal degradation (Figure 1).[1,2] Inhibition of this interaction upregulates the LDLR and leads to a drastic lowering of LDL and the risk of heart disease, making it the most attractive new target for lowering LDL-cholesterol. Two anti-PCSK9 monoclonal antibodies (mAb), Evolocumab and Alirocumab, were recently approved by FDA.[3,4] By disrupting the PCSK9-LDLR interaction, these mAbs can reduce over 60% LDL-cholesterol in patients. However, antibodies require injection and they are much more expensive than small molecules. Peptides that mimic the epidermal growth factor precursor homology domain A (EGF-A) domain of the LDLR[5–13], PCSK9 antisense oligonucleotides[14–18] and RNAi of PCSK9[19–21] are also under development, though they have the same limitations as antibodies with respect to cost and oral availability. Small molecules have the potential to overcome these limitations and have the flexibility to be tuned for desired pharmacological properties[22,23].

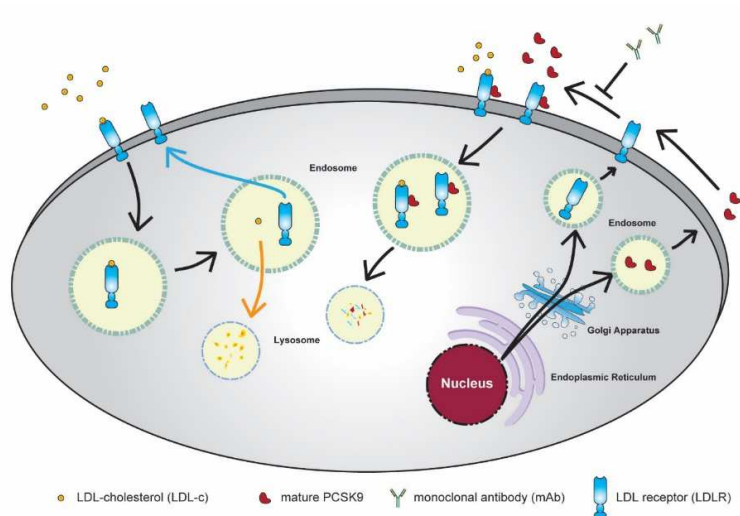


Figure 1. PCSK9 mediated lysosomal degradation of LDLR

Phenotypic screening and target-based screening are two of the major approaches for drug discovery. Target based screening allows for more rational design as results in biochemical assays are easier to interpret, especially after the target-ligand interactions are fully characterized.[24] Phenotypic screening led to the discovery of a number of first-in-class drugs in history.[25] It has attracted more and more interest from both industry and academic in recent years[26,27] across many areas of diseases.[28–31] Phenotypic screening aimed at inhibition of PCSK9 protein production is a promising approach for the discovery of small molecule PCSK9 inhibitors or modulators. Berberine (BBR),[32,33] tetrahydroprotoberberine derivatives (*R*)-22,[34] difluoro-2,3'-diindolymethane (DFDIM, **1**),[35] 7030B-C5[36] and BRD8518[37] were discovered with the activity of reduction of secreted PCSK9 protein (Figure 2). R-IMPP showed a novel molecular mechanism of action (MoA) that targeted the 80S ribosome and inhibited PCSK9 protein translation, and was discovered by phenotypic screening in a CHO-K1 cell line overexpressing recombinant ProLabel-tagged PCSK9.[38] PF-06446846, an analogue of R-IMPP, was subsequently developed with improved pharmaceutical properties.[39] By directly targeting PCSK9 protein, a number of small molecules were developed, including LDLL-1dlnr[40] and 3f[41] that disrupts the interaction of PCSK9 and LDLR, Heparin oligosaccharide (e.g. Heparin I) that prevents the recruitment of PCSK9 to LDLR via heparan sulfate proteoglycans (HSPG) on cell membrane,[42] and a PCSK9 degrader using CMPD9 as the ligand.[43]

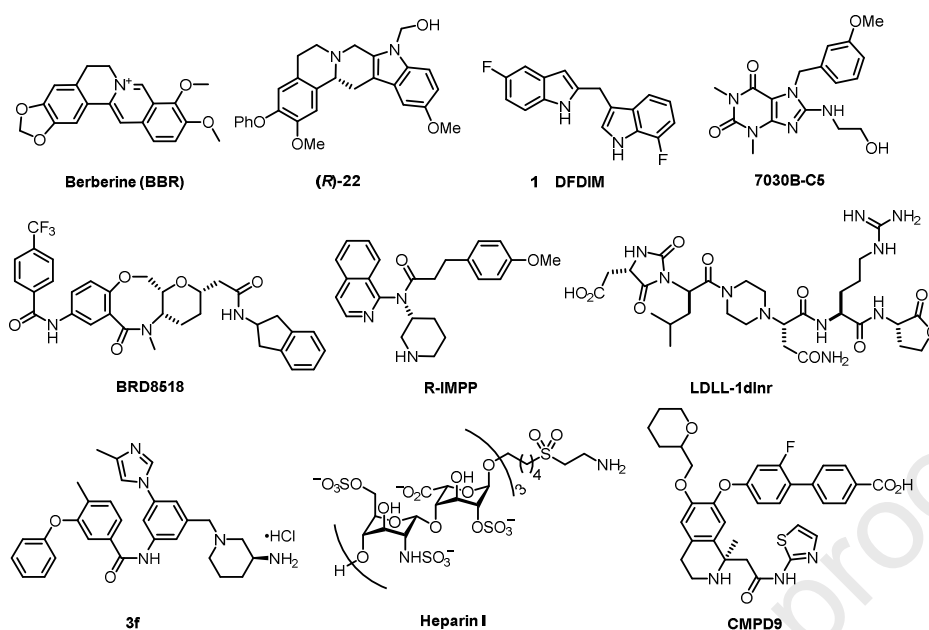


Figure 2. Small-molecule PCSK9 modulators derived from phenotypic screening: BBR, (R)-22, DFDIM, 7030B-C5, BRD8518 and R-IMPP; Small-molecule PCSK9 inhibitors or binders derived from targeted-based approach: LDLL-1dlnr, 3f, Heparin I and CMPD9.

Results and Discussion

Previously, we have discovered a class of small-molecules with a DIM skeleton that can decrease the expression of PCSK9 with sub-micromolar IC_{50} s in HepG2 cells.[35] After performing preliminary structure–activity relationship (SAR) optimization, the PCSK9 inhibitor DFDIM **1** with 202 ± 78 nM IC_{50} was developed. In HepG2 cells, compound **1** decreased PCSK9 protein levels in both cell lysate and media as measured by sandwich ELISA. While working on the elucidation of the mechanism of action (MoA) and target identification of **1**, we also performed a systematic SAR investigation based on the structure of **1** to obtain more potent, soluble, and metabolically stable analogues for *in vivo* pharmacokinetics and future proof-of-concept efficacy studies. However, unlike target-based SAR studies, phenotype-based SAR studies are more challenging due to multiple factors that can impact the activity of the compounds. In addition to the potency for decreasing PCSK9 protein level, we also optimized the liver microsomal stability of the compounds as liver is the primary tissue we need to target and compound **1** has obvious metabolic liability.

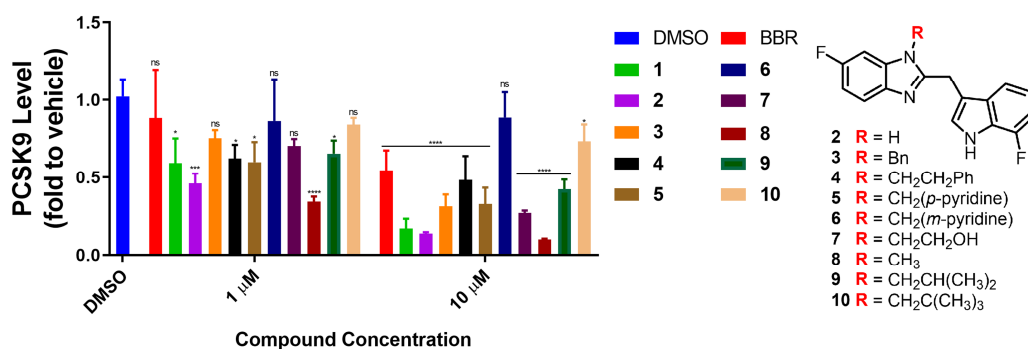


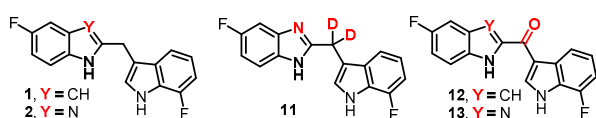
Figure 3. SAR of *N*-substitutions of benzimidazole. HepG2 cells were treated with compounds at various concentrations for 48 h. Medium sample were analyzed by human PCSK9 ELISA. Data was normalized to vehicle (DMSO) treated group and bar graph represented as mean of relative PCSK9 protein level (n = 3) with \pm SD as error bar. Statistical significance was analyzed by one-way ANOVA in comparison with vehicle (DMSO) treated group. Not significant (ns), * $p \leq 0.05$, *** $p \leq 0.001$, **** $p \leq 0.0001$.

Replacement of a CH motif by its isostere N often retains the activity while improving the metabolic stability and solubility.[44,45] We initiated our optimization by the design of difluorobenzoimidazolylindolylmethane (DFBIIM) **2** because of its ease of synthesis and also the flexibility to introduce various R groups to the nitrogen of the benzoimidazole ring, including both small/bulky and non-polar/polar substituents. The substituted group on the N atom of benzimidazole was systematically explored (Figure 3). Among the diverse range of substituents, the addition of a methyl group to the parent compound **2** significantly improved the potency of compound **8**, a classical “methyl effect”.[46,47]

We suspected that the methylene group between the two indoles in **1**, or between the benzoimidazole and indole in **2** or **8**, would be one of the most metabolically labile sites, because they are activated by two adjacent aryl rings towards potential oxidative reactions. Replacement of one or more hydrogens by isotopic deuterium can often increase the metabolic stability, while retaining the biological activity. In 2017, the first deuterated drug, deutetrabenazine, was approved by US FDA.[48–51] Longer half-life and the reduction of toxic metabolites are the major advantages of deuterated drugs.[52,53] Analogue **11** was designed and synthesized by deuterating the potential metabolically labile methylene group. We then thoroughly examined the metabolic stability of PCSK9 modulators **1** and **2** across three different species to establish the correlation among mice, rat, and human (Table 1). Both compounds **1** and **2** are

indeed relatively metabolically labile, compared to their analogues in the same series. The half-life in human is generally 2-4 times longer than those in mice and rats. The metabolic stability of **11** was increased over two times compared to compound **2** in both mice and rats. For example, the half-life of **11** in mice was increased from 7.2 to 16.3 minutes, suggesting that the methylene bridge is indeed a metabolically labile sites as we suspected. From these results, we further converted the methylene group of compounds **1** and **2** to carbonyl group by SeO₂. The metabolic stability of ketones DFDIK **12** and DFBIK-1 **13** in both mice and rats was increased significantly over compounds **1** and **2**, respectively.

Table 1. Microsomal stability of potential PCSK9 modulators



Compound	Human Liver Microsomal Stability		Mice Liver Microsomal Stability		Rat Liver Microsomal Stability	
	T _{1/2} (min)	CL _{int} (μL/min/mg)	T _{1/2} (min)	CL _{int} (μL/min/mg)	T _{1/2} (min)	CL _{int} (μL/min/mg)
1	63.9±15.0	23.0±5.5	16.5±0.2	83.9±1.1	23.2±2.8	60.7±7.8
2	17.5±0.2	79.4±1.0	7.1±0.3	194.9±9.5	9.5±0.1	145.6±1.3
11	-	-	16.3±0.3	85.2±1.8	23.5±1.1	59.1±3.0
12	-	-	40.1±2.2	34.6±1.8	76.9±5.8	18.1±1.4
13	-	-	30.0±2.5	46.5±4.0	47.8±5.8	29.4±3.3
14	-	-	25.8±2.9	54.6±6.6	42.4±2.9	33.1±3.6

It is not clear if the change of a methylene bridge in **1** and **2** to a ketone bridge in **12** and **13**, respectively, would have any effect on the activity towards lowering PCSK9 protein level. We then compared the activity of **12** and **13** with **1** and **2** for their ability to decreased PCSK9 secretion from HepG2 cells (Figure 4). We were pleased that compounds **12** and **13** have much higher potency than their counterparts **1** and **2** at 1 μM concentration. Nearly 90% reduction of PCSK9 protein was observed with 1 μM of PCSK9 modulator **13**.

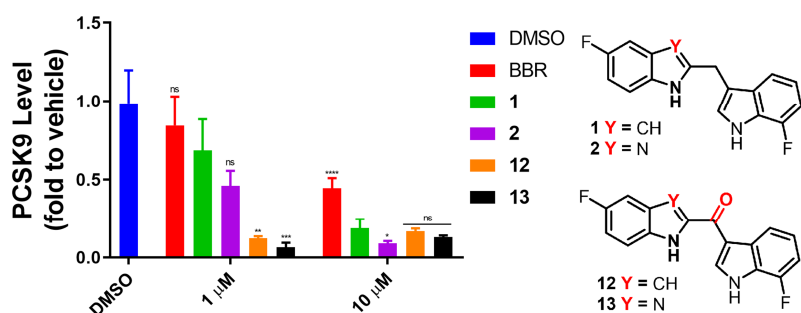


Figure 4. SAR of compounds with methylene or ketone linkages. HepG2 cells were treated with compounds at various concentrations for 48 h. Medium sample were analyzed by human PCSK9 ELISA. Data was normalized to vehicle (DMSO) treated group and bar graph represented as mean of relative PCSK9 protein level ($n = 3$) with \pm SD as error bar. Statistical significance was analyzed by one-way ANOVA in comparison with compound 1 treated group at same concentration. Not significant (ns), $*p \leq 0.05$, $**p \leq 0.01$, $***p \leq 0.001$, $****p \leq 0.0001$.

Having two potent PCSK9 modulators with much higher metabolic stability, we decided to establish the correlation of *in vivo* pharmacokinetics with the *in vitro* metabolic stability (Table 2). The preliminary *in vivo* pharmacokinetic study for compounds **12** and **13** were performed in mice. Mice were intraperitoneally injected with 6 mg/kg of **12** or **13**. Plasma samples were collected and analyzed by LC-MS/MS. Both compounds reached their peak concentrations of about 1.0 μ M near 15 minutes after injection (Table 2). We performed one-phase-decay nonlinear fitting of all biological and technical replicates and obtained the plasma half-life ($T_{1/2}$) and other parameters of these two compounds. The $T_{1/2}$ of **12** and **13** were 1.31 and 1.64 hours, respectively. The trend of the *in vivo* data for compounds **12** and **13** correlate well with their *in vitro* metabolic stability. These results thus provide valuable information for further optimization and *in vivo* studies.

Table 2. Preliminary pharmacokinetic study DFDIK **12** and DFBIK-1 **13** in mice^a

	12	13
Route of administration	IP	IP
Dose (mg/kg)	6.0	6.0
AUC _{0-∞} (μ g/L•h) ^b	610.3	695.6

C_{\max} ($\mu\text{g/L}$) ^c	322.9 ± 23.7	294.3 ± 8.9
$T_{1/2}$ (h) ^d	1.31	1.64

a. Compounds were formulated in DMSO (10 %) and Tween 80 (10 %) in PBS (80 %).

b. $AUC_{0-\infty}$, total exposure following a single dose.

c. C_{\max} , maximum plasma concentration following a single dose.

d. $T_{1/2}$, half-life.

Incorporation of fluorine is a common strategy in drug discovery. About 20% of FDA approved drugs contain at least one fluorine atom across many different drug classes.[54–56] Fluorine substitutions not only modulate the ADME profiles but also impact protein-ligand binding affinity.[57–61] A systematic fluorine scan on ligands has become a routine approach in hit-to-lead optimization strategies.[62,63] We previously performed a fluorine scan for the parent diindolylmethane **1**.[35] In order to examine the effect of the two fluorine atoms on the A-ring and D-ring of compound **13**, we prepared their parent analogue **14**, analogues **15** and **16**, which lack one of the two fluorine atoms, and analogue **17**, which has the fluorine on the 4-position instead of 5-position. The potency of those analogues was compared at three different concentrations (Figure 5A). Each fluorine atom on either A-ring or D-ring slightly improved the potency and two fluorine atoms cooperatively improved the potency further. The position of fluorine on A-ring does not significantly impact the activity for PCSK9 modulation. We then compared the microsomal stability of compounds **13** and **14** (Table 1). The two fluorine atoms in compound **13** improved its metabolic stability in both mice and rats over the parent compound **14** without two fluorine atoms.

We then conducted a systematic fluorine scan SAR studies for analogues with the ketone linkage and an additional methyl group on the benzoimidazole nitrogen (Figures 6B and 6C), because of the “methyl effect” we observed for the improved potency of compound **8** over its parent compound **2**. No significant difference was observed for the PCSK9 modulation activity among the five compounds, including compound **18** without the fluorine in the benzoimidazole ring and compounds **19-22** with the fluorine at different positions (Figure 5B). On the other hand, the position of the fluorine atom on the indole ring significantly impacted activity (Figure 5C). Compared to compound **23** without the fluorine on the D-ring, fluorine substitution on the 5 and 4 positions decreases the potency, whereas fluorine

substitution on the 6 and 7 positions increases the potency. The SAR trend of the fluorine scan on the D-ring of compound **2** is very similar to the trend of the fluorine scan observed for the original hit compound **1**,^[35] suggesting that these two classes of compounds have the same mechanism of action. Compound **21** has the most significant PCSK9 modulation activity at both 10 and 100 nM concentrations ($35.0\% \pm 4.4\%$ and $12.5\% \pm 2.1\%$ reduction of PCSK9, respectively), though compound **20** showed similar potency ($34.4\% \pm 2.7\%$ and $11.9\% \pm 0.3\%$ reduction of PCSK9 at 10 and 100 nM, respectively).

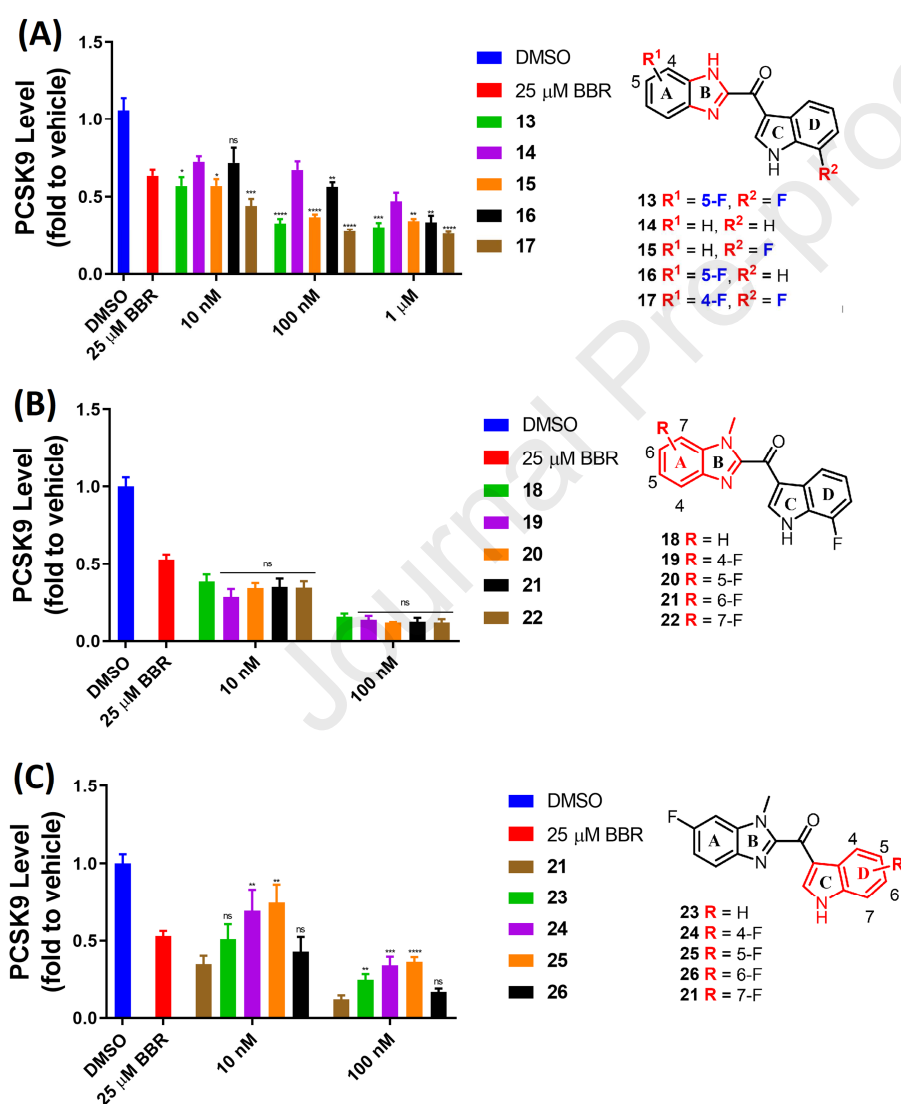


Figure 5. Fluorine scan SAR of carbonyl linked analogues. (A) Fluorine substitution on A-ring and D-ring of carbonyl linked benzimidazoleindole; (B) ‘F-scan’ SAR of A-ring carbonyl linked N-methyl-

benzimidazoleindole (C) ‘F-scan’ SAR of D-ring of *N*-methyl-benzimidazoleindole. HepG2 cells were treated with compounds at various concentrations for 48 h. Medium sample were analyzed by human PCSK9 ELISA. Data was normalized to vehicle (DMSO) treated group and bar graph represented as mean of relative PCSK9 protein level ($n = 3$) with \pm SD as error bar. Statistical significance was analyzed by one-way ANOVA in comparison with compound 14- (A), 18- (B) or 21- (C) treated group at same concentration. Not significant (ns), $*p \leq 0.05$, $**p \leq 0.01$, $***p \leq 0.001$, $****p \leq 0.0001$.

We then further compared the microsomal stability of compounds **13** and **21** (Figure 6). The methyl group in compound **21** clearly improved its metabolic stability in both mice and rats over the parent compound **13** without the methyl group.

We further examined the full dose-response of compounds **2**, **13** and **21** for PCSK9 modulation and compared their potency with metabolic stability in Figure 6. The effect of *N*-methylation and carbonyl linker replacement on activity is dramatic. The potency was improved 139-fold by the carbonyl linker replacement in compound **13** and 17-fold by *N*-methylation on compound **21**. A total of 2,320-fold increased potency was achieved by two relatively simple modifications. The metabolic stability was also increased by the two modifications as summarized in Figure 6.

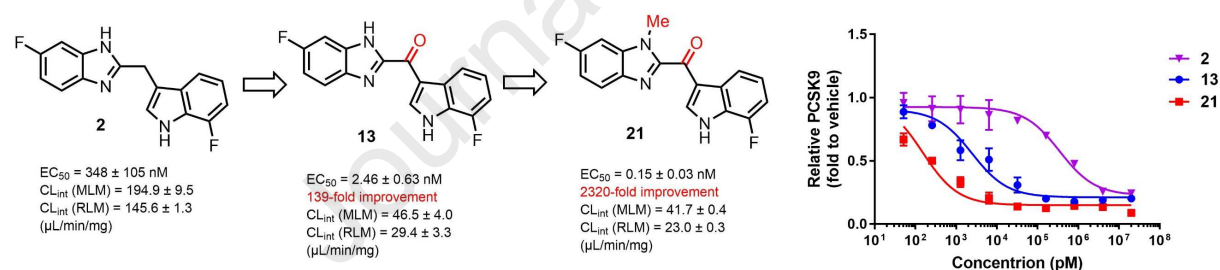


Figure 6. The effect of *N*-methylation and carbonyl linker replacement on potency and microsomal stability. HepG2 cells were treated with compounds at various concentrations for 48 h. Medium sample were analyzed by human PCSK9 ELISA. Data was normalized to vehicle (DMSO) treated group and dot plot represented as mean of relative PCSK9 protein level ($n = 3$) with \pm SD as error bar. The dose response curve was fitted using “log(inhibitor) vs. response (three parameters)” by GraphPad Prism.

To facilitate the mechanism of action studies, it is important to identify a position within the compound that can be modified without significantly interfering with the biological activity. Such a position may also help to further improve other pharmacological properties. Analogues with an *N*-substituent on either the benzimidazole ring or the indole ring are more synthetically accessible than those with substituents

on the benzene ring. We first prepared compounds **27-29** with different *N*-alkyl substituents on the benzimidazole ring or the indole ring and compared their activity for PCSK9 modulation at three different concentrations (Figure 7). Clearly, the R¹ position cannot tolerate a large substituent. This is what we expected based on SAR studies shown in Figure 3. Conversely, a large substituent on the R² position can be well tolerated as shown by the activity of compound **28**, though the activity was decreased at lower concentrations.

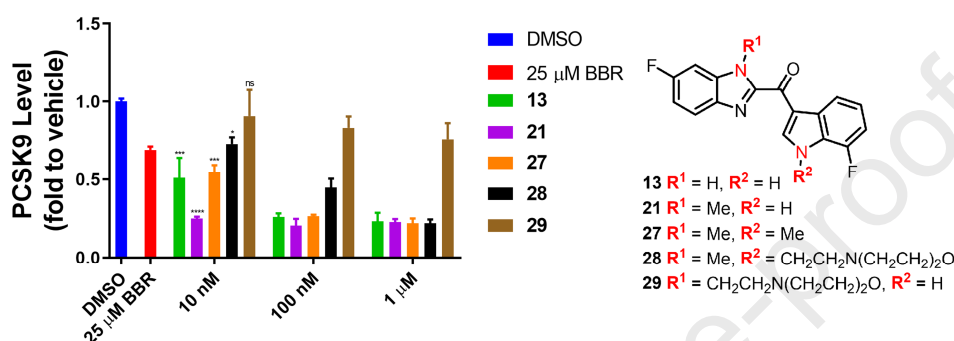
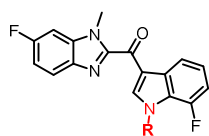


Figure 7. Investigation of the effect of *N*-substituent on the benzimidazole and indole. HepG2 cells were treated with compounds at various concentrations for 48 h. Medium sample were analyzed by human PCSK9 ELISA. Data was normalized to vehicle (DMSO) treated group and bar graph represented as mean of relative PCSK9 protein level ($n = 3$) with \pm SD as error bar. Statistical significance was analyzed by one-way ANOVA in comparison with vehicle (DMSO) treated group. Not significant (ns), $*p \leq 0.05$, $***p \leq 0.001$, $****p \leq 0.0001$.

We then further conducted a dose response studies for analogues with various R-group on the indole nitrogen (Table 3). Although all these analogues are less potent than the parent compound **21**, compounds **32** and **33** showed very promising activity with EC₅₀ values less than 1 nM. The activity of compounds **28**, **30**, and **31** was lower than the parent compound **21**, when the morpholine was introduced with an alkyl linker. Interestingly, most of the activity could be retained in compound **33**, when the morpholine was introduced with a sulfonamide alkyl linker. Replacement of the morpholine ring in **33** by a piperidine ring in **34** significantly reduced the activity. Derivatives of compounds **32** and **33** will be prepared in the near future for target identification and the studies of mechanism of action. At the same time, an appropriate animal model will be identified for the investigation of the full pharmacokinetic profile and *in vivo* efficacy of this class PCSK9 modulators.

Table 3. SAR of substitutions on the nitrogen of indole^a



Compound	R	EC ₅₀ (nM)
21		0.15±0.03
27		1.21±0.34
28		11.0±3.5
30		39.9±19.0
31		88.0±25.0
32		0.28±0.06
33		0.69±0.21
34		161±32

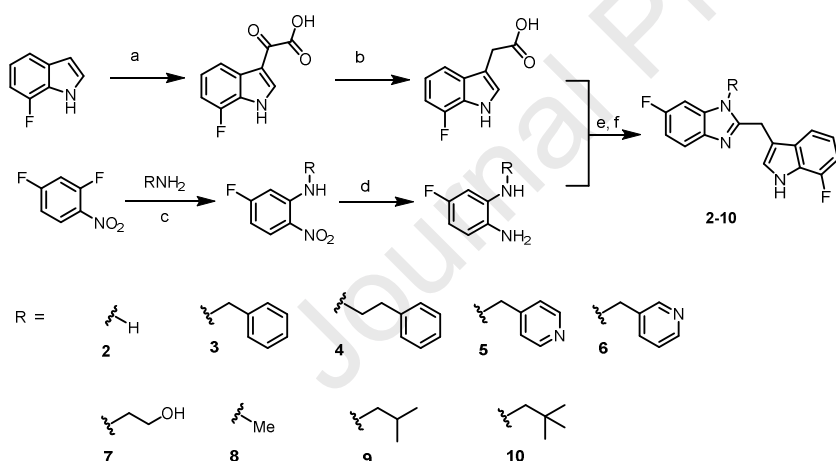
a. Dose response curve (See Figure S1).

During our previous studies,[35] we checked the cytotoxicity of the DIM compounds to ensure the reduction of PCSK9 was not due to cell death. No compounds showed any obvious cytotoxicity at concentrations of 10 μ M or lower. We also analyzed the cytotoxicity of all the improved analogues by MTT assay at 1.0 μ M (See Figure S2). At this concentration, the maximal PCSK9 reduction could be achieved and most compounds did not show any obvious cytotoxicity. We can conclude that the reduction of PCSK9 by these new analogues with much higher potency is not due to cytotoxicity.

The syntheses of compounds **2-34** are summarized in Schemes 1-4. Commercially available 7-fluoroindole was acylated by Friedel–Crafts reaction using oxalyl chloride. After hydrolysis and Wolff-Kishner-Huang reduction, the 7-fluoroindole-3-acetic acid product was obtained. Based on the same

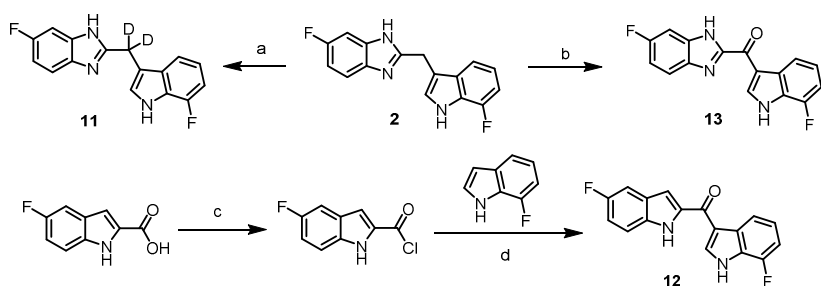
procedure, 4, 5 and 6-F substituted isomers were prepared. The 2-fluorine of 2,4-difluoronitrobenzene was substituted by a variety of primary amines through a S_NAr reaction. After reduction, a series of desired *N*-substituted *o*-phenylenediamines were prepared. According to a similar procedure, 5-fluoro and 3-fluoro *N*¹-methylbenzene-1,2-diamines were prepared from 2,4-difluoronitrobenzene and 2,6-difluoronitrobenzene, respectively. The other two isomeric 4-fluoro and 6-fluoro *N*¹-methylbenzene-1,2-diamines were prepared from 2,4-difluoronitrobenzene and 2,6-difluoronitrobenzene, respectively, through additional Boc protection, *N*-methylation and deprotection steps. The two intermediates, indole-3-acetic acids and benzene-1,2-diamines, were then coupled by EDCI and HOBt, followed by intramolecular condensation, to afford the methylene linked analogues.

The deuterated analogue **11** was easily prepared from compound **2** by H-D exchange in DMSO- d_6 /D $_2$ O. The linker methylene group can also be oxidized to carbonyl by SeO $_2$ and afforded the corresponding carbonyl bridged analogues. The additional substituents on the nitrogen of the indole ring were introduced by straightforward alkylation reactions.



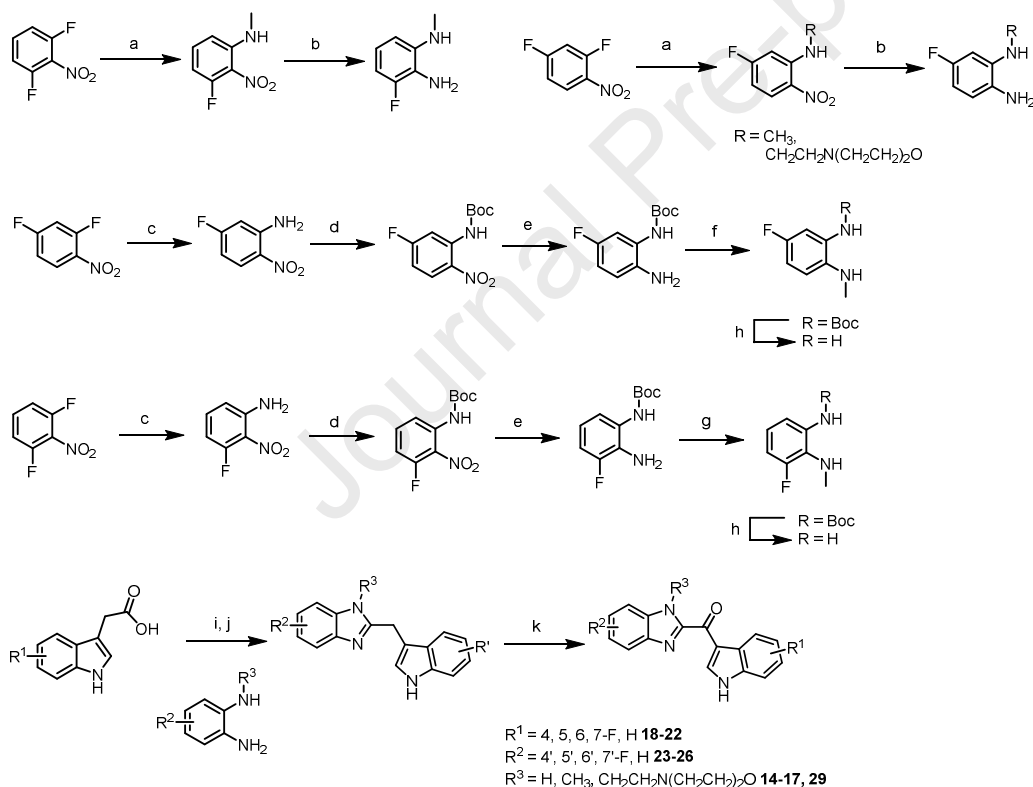
Reagents and conditions: (a) oxalyl chloride (1.2 equiv), NaHCO $_3$, Et $_2$ O; (b) hydrazine hydrate (5.0 equiv), NaOH, ethylene glycol, 150 °C (c) DIPEA (2.0 equiv), DMSO, 0 °C to rt, 15hrs, >95%; (d) Pd/C, H $_2$ (1.0 atm), MeOH, rt, 80%; (e) EDCI, HOBt, DMF, rt; (f) Toluene/AcOH (2/1), Microwave, 150 °C, d, e total yield 70%.

Scheme 1. Synthesis of Compounds 2-10



Reagents and conditions: (a) Microwave, DMSO-*d*₆/D₂O, 160 °C, yield > 95%; (b) SeO₂, 1,4-dioxane, 100 °C, yield 71% (c) SOCl₂, DMF (cat.), Et₂O, rt; (d) SnCl₄ (1.3 equiv), DCM/MeNO₂, rt; d, e total yield 31%.

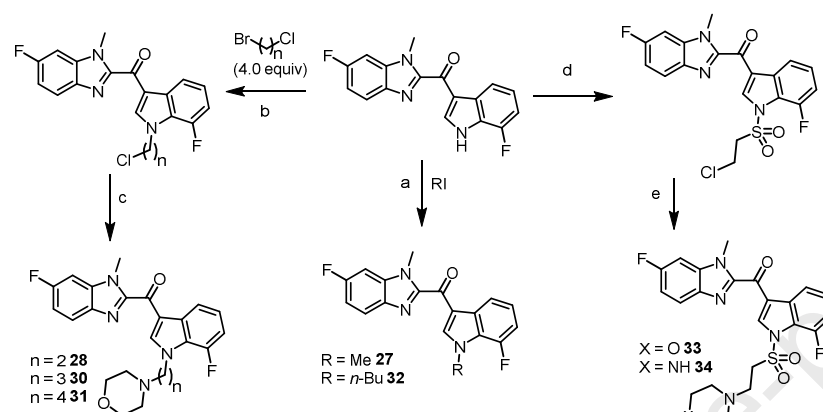
Scheme 2. Synthesis of Compounds 11, 12 and 13



Reagents and conditions: (a) MeNH₂, DIPEA, DMSO, 0 °C to rt, yield 95%; (b) Fe, NH₄Cl, EtOH/H₂O, 80 °C, yield 80%; (c) NH₃•H₂O, DIPEA, DMSO, 0 °C to rt, yield 95%; (d) 1) DMAP (10 mol %), Boc₂O (2.2 equiv), DMF, rt, 2) TFA 3.2% in DCM, yield 95%; (e) Pd/C 10%, H₂ (1.0 atm), MeOH, rt, yield 80% (f) MeI (1.0 equiv), Na₂CO₃, DMF, rt, yield 40%; (g) MeB(OH)₂, Cu(OAc)₂, Pyridine, 1,4-

dioxanes, 100 °C, yield 60%; (h) TFA 50 vol. % in DCM, rt, yield 90% (i) HOBt, EDCl, DMF, rt; (j) AcOH/Toluene, Microwave, 150 °C; (k) SeO₂ (2.0 equiv), 1,4-dioxanes, 100 °C; total yield of (i), (j) and (k) 50%.

Scheme 3. Synthesis of Compounds 14-26 and 29



Reagents and conditions: (a) MeI (3.0 equiv) or *n*-BuI (3.0 equiv), Cs₂CO₃ (1.5 equiv), Acetonitrile, rt, yield >95%; (b) K₂CO₃ (4.0 equiv), Acetone, 70 °C, yield 85%; (c) Morpholine, TBAI (0.2 equiv), 100 °C, yield 80%; (d) NaH (1.2 equiv), ClSO₂CH₂CH₂Cl (1.5 equiv), DMF, 0 °C to rt, yield 70%; (e) Morpholine (10.0 equiv) or Piperazine (10.0 equiv), TBAI (0.2 equiv), DMSO, 110 °C, yield 70%.

Scheme 4. Synthesis of Compounds 27, 28 and 30-34

Conclusions

In summary, based on our previously developed PCSK9 modulator DFDIM **1** (EC₅₀ = 200 nM), a series of analogues were designed and synthesized to further improve the potency and metabolic stability. Our initial SAR studies for the substituents in DFBIIM **2** indicated that the addition of a methyl substituent to the nitrogen of the benzimidazole ring in **8** greatly improved its potency. After investigating the liver microsomal stability for compounds **1** and **2** in different species, we hypothesized that the methylene bridge between the two heterocycles in DFDIM or DFBIIM may be a metabolically labile site. In order to validate this hypothesis, deuterated compound **11** was prepared. The improved metabolic stability of **11** over **2** supports the above hypothesis. We then prepared carbonyl linked bisindole DFDIK **12** and benzoimidazole-indole DFBIK-1 **13**. We found that these two compounds had not only much better metabolic stability, but also nearly 100-fold higher potency. These data prompted us to initiate the

preliminary PK study in mice to establish a correlation between *in vitro* metabolic stability and *in vivo* PK performance of this class of PCSK9 modulators. During subsequent optimizations, we introduced the methyl substituent to the benzimidazole nitrogen of DFBIK-1 **13** and prepared DFBIK-2 **21**, which yielded an additional 17-fold increase of potency. To systematically investigate the effect of the two fluorine substituents on the ketone linked benzoimidazole-indoles, an 'F-scan' was also conducted on both heterocycles. In addition, we also investigated the effect of different substituents on each of the two nitrogen atoms in the benzoimidazole and indole heterocycles, respectively. We found that the nitrogen of indole can tolerate various substituents, which may be useful for future target identification and mechanism of action studies, which will be reported in due course.

Experimental Sections

General Information in Synthetic Chemistry

All reactions were conducted under a positive pressure of dry argon in a glassware that had been oven-dried prior to use. Anhydrous solutions of reaction mixtures were transferred via an oven-dried syringe or cannula. All solvents were dried prior to use unless noted otherwise. Thin-layer chromatography (TLC) was performed using precoated silica gel plates. Flash column chromatography was performed with the silica gel. ^1H and ^{13}C nuclear magnetic resonance (NMR) spectra were recorded on Bruker 400, 500, 600 MHz and Varian 500 MHz spectrometers. ^1H NMR spectra were reported in parts per million (ppm) referenced to 7.26 ppm of CDCl_3 or referenced to the center line of a septet at 2.50 ppm of $\text{DMSO-}d_6$. Signal splitting patterns were described as singlet (s), doublet (d), triplet (t), quartet (q), quintet (quint), or multiplet (m), with coupling constants (J) in hertz. High-resolution mass spectra (HRMS) were performed on an electron spray injection (ESI) TOF mass spectrometer. The liquid chromatography–mass spectrometry (LC–MS) analysis of final products was processed on an Agilent 1290 Infinity II LC system using a Poroshell 120 EC-C18 column (5 cm \times 2.1 mm, 1.9 μm) for chromatographic separation. Agilent 6120 Quadrupole LC/MS with multimode electrospray ionization plus atmospheric pressure chemical ionization was used for detection. The mobile phases were 5.0% methanol and 0.1% formic acid in purified water (A) and 0.1% formic acid in methanol (B). The gradient was held at 5% (0–0.2 min), increased to 100% at 2.5 min, then held at isocratic 100% B for 0.4 min, and then immediately stepped back down to 5% for 0.1 min re-equilibration. The flow rate was set at 0.8 mL/min. The column temperature was set at 40 $^\circ\text{C}$. The purities of all of the final compounds

were determined to be over 95% by LC–MS. See the Supporting Information for ^1H and ^{13}C NMR spectra and LC–MS purity analysis of all compounds.

General procedure for the preparation of compounds **2-10**.

In a 250 mL flask with a magnetic stirring bar, 7-fluoroindole (2.0 g, 14.8 mmol) was dissolved in 50 mL ethyl ether and cooled by ice-water bath. Oxalyl chloride (2N DCM solution) (8.9 mL, 17.8 mmol) was added by dropping funnel. Half of an hour later, the empty dropping funnel and ice-water bath were removed, and the reaction mixture was stirred at room temperature for another 5 h. Then the reaction mixture was quenched by NaHCO_3 saturated solution and stirred overnight. After carefully adjusting to pH 1.0 by 1N HCl, the organic phase was separated, and the aqueous phase was extracted by 100 mL ethyl acetate. The organic phase was combined and dried by Na_2SO_4 , then the solvent was removed by rotavapor to yield 3.06 g of solid, which was directly used for the next step reaction.

In a 250 mL flask with a magnetic stirring bar, the 3.06 g of solids, hydrazine hydrate (3.7 g, 74.0 mmol) and sodium hydroxide (6.5 g, 162.8 mmol) were suspended in 35 mL ethylene glycol. The reaction mixture was heated to 60 °C for half an hour, then heated to 150 °C for another 4 h. After cooling to room temperature, the reaction mixture was adjusted to pH 1.0 by 1N HCl, extracted by 100 mL ethyl acetate twice. The organic phase was combined and dried by Na_2SO_4 , the solvent was then removed by rotavapor, the residue was purified by silica gel column chromatography (eluted with methanol in DCM from 0.5% to 5%) and 2.0 g of 7-fluoroindole-3-acetic acid was prepared (two steps, total yield of 70%).

In a 150 mL flask with a magnetic stirring bar, 2,4-difluoronitrobenzene (1.0 g, 6.29 mmol) and DIPEA (1.6 g, 12.58 mmol) were suspended in 10 mL DMSO and cooled in ice-water bath, then benzyl amine (0.67 g, 6.29 mmol) was added to the reaction mixture. After stirring overnight, the reaction mixture was quenched by 100 mL NaHCO_3 saturated solution. The yellow precipitate was collected by filtration and washed by 50 mL water three times and 50 mL hexane twice. After drying by high vacuum, 1.5 g of yellow solid was generated.

In a 100 mL flask with a magnetic stirring bar, *N*-benzyl-5-fluoro-2-nitroaniline (0.5 g, 2.03 mmol) and Pd/C (100 mg) were suspended in 15 mL methanol. After sealing by rubber stopper, a 2.0 L hydrogen balloon was connected with the reaction flask by a syringe needle. The reaction mixture was then stirred overnight at room temperature. After removing the Pd/C by filtration, the solvent was removed by rotavapor. The residue was then purified by silica gel column chromatography to afford 352 mg of *N*¹-benzyl-5-fluorobenzene-1,2-diamine (80% yield).

In a 10 mL flask with a magnetic stirring bar, a mixture of *N*¹-benzyl-5-fluorobenzene-1,2-diamine (118 mg, 0.54 mmol), 7-fluoroindole-3-acetic acid (100 mg, 0.52 mmol), HOBt hydrate (79 mg, 0.52 mmol), EDCI (149 mg, 0.78 mmol) and DMF (2.5 mL) were stirred at room temperature for 5.0 h. The reaction mixture was then poured to 100 mL ethyl acetate and washed by 100 mL NaHCO₃ saturated aqueous solution three times. The organic phase was dried by Na₂SO₄, the solvent was then removed by rotavapor. The residue was suspended in toluene /AcOH (4 mL/2 mL) and heated at 150 °C by microwave for 1.0 h. After cooling to room temperature, the reaction mixture was then poured to 100 mL ethyl acetate, washed by 100 mL NaHCO₃ saturated aqueous solution three times. The organic phase was dried by Na₂SO₄, the solvent was then removed by rotavapor. The residue was then purified by silica gel column chromatography to yield 148 mg of compound **3** (76% yield).

6-fluoro-2-((7-fluoro-1H-indol-3-yl)methyl)-1H-benzo[d]imidazole(2) ¹H NMR (400 MHz, Chloroform-*d*) δ 8.72 (s, 1H), 7.35 (dd, *J* = 8.8, 4.6 Hz, 1H), 7.21 – 7.16 (m, 1H), 7.15 – 7.09 (m, 2H), 6.97 – 6.87 (m, 3H), 4.34 (s, 2H). HRMS (ESI) calcd for C₁₆H₁₁F₂N₃ (M + Na)⁺ 306.0813, found 306.0816. LC-MS Purity: 98.4 %, R_t = 2.06 min.

1-benzyl-6-fluoro-2-((7-fluoro-1H-indol-3-yl)methyl)-1H-benzo[d]imidazole (3) ¹H NMR (400 MHz, Chloroform-*d*) δ 8.37 (s, 1H), 7.71 (ddd, *J* = 8.9, 4.8, 0.5 Hz, 1H), 7.30 – 7.27 (m, 1H), 7.25 – 7.19 (m, 3H), 7.03 – 6.94 (m, 3H), 6.91 – 6.83 (m, 4H), 5.20 (s, 2H), 4.35 (d, *J* = 1.1 Hz, 2H). ¹³C NMR (101 MHz, Acetone-*d*₆) δ 160.0 (d, *J* = 236.4 Hz), 155.5 (d, *J* = 3.2 Hz), 150.5 (d, *J* = 242.5 Hz), 140.3, 137.3, 137.0 (d, *J* = 13.4 Hz), 132.2 (d, *J* = 5.6 Hz), 129.4, 128.3, 127.2, 125.4, 125.2, 120.7 (d, *J* = 10.2 Hz), 112.0 (d, *J* = 6.2 Hz), 115.9 (d, *J* = 3.4 Hz), 111.7 (d, *J* = 2.4 Hz), 110.2 (d, *J* = 25.1 Hz), 107.0 (d, *J* = 16.2 Hz), 97.6 (d, *J* = 27.9 Hz), 47.8, 25.5. HRMS (ESI) calcd for C₂₃H₁₇F₂N₃ (M + H)⁺ 374.1463, found 374.1460. LC-MS Purity: 98.6 %, R_t = 2.74 min.

6-fluoro-2-((7-fluoro-1H-indol-3-yl)methyl)-1-phenethyl-1H-benzo[d]imidazole (4) ¹H NMR (400 MHz, Chloroform-*d*) δ 8.36 (s, 1H), 7.68 (ddd, *J* = 8.7, 4.8, 0.5 Hz, 1H), 7.27 – 7.23 (m, 4H), 7.04 – 6.87 (m, 5H), 6.85 – 6.80 (m, 2H), 4.17 (t, *J* = 7.2 Hz, 2H), 3.99 (d, *J* = 1.1 Hz, 2H), 2.79 (t, *J* = 7.2 Hz, 2H). ¹³C NMR (101 MHz, Chloroform-*d*) δ 159.5 (d, *J* = 239.1 Hz), 154.2 (d, *J* = 2.9 Hz), 149.6 (d, *J* = 244.5 Hz), 138.8, 137.5, 135.2 (d, *J* = 13.0 Hz), 130.6 (d, *J* = 5.5 Hz), 128.9, 128.7, 127.1, 124.7 (d, *J* = 13.5 Hz), 123.4, 120.1 (d, *J* = 10.1 Hz), 120.0 (d, *J* = 6.1 Hz), 114.5 (d, *J* = 3.4 Hz), 111.3 (d, *J* = 2.3 Hz), 110.2 (d, *J* = 24.9 Hz), 107.1 (d, *J* = 16.0 Hz), 96.2 (d, *J* = 27.5 Hz), 45.9, 35.5, 24.5. HRMS (ESI) calcd for C₂₄H₁₉F₂N₃ (M + H)⁺: 388.1620, found 388.1618. LC-MS Purity: 96.3 %, R_t = 2.73 min.

6-fluoro-2-((7-fluoro-1H-indol-3-yl)methyl)-1-(pyridin-4-ylmethyl)-1H-benzo[d]imidazole (5) ¹H NMR (400 MHz, Methanol-*d*₄) δ 8.18 (s, 1H), 8.07 – 8.03 (m, 2H), 7.72 – 7.67 (m, 1H), 7.20 – 7.17 (m, 1H), 7.10 – 7.00 (m, 3H), 6.89 – 6.82 (m, 1H), 6.78 – 6.72 (m, 1H), 6.54 – 6.50 (m, 2H), 5.48 (s, 2H), 4.47 (s, 2H). ¹³C NMR (101 MHz, Methanol-*d*₄) δ 161.3 (d, *J* = 239.2 Hz), 156.7, 151.0 (d, *J* = 243.6 Hz), 149.5, 147.3, 139.1, 137.2 (d, *J* = 13.2 Hz), 132.2 (d, *J* = 5.8 Hz), 126.1, 125.9, 122.2, 120.6 (d, *J* = 10.2 Hz), 120.5 (d, *J* = 6.2 Hz), 115.4 (d, *J* = 3.5 Hz), 111.9 (d, *J* = 25.5 Hz), 110.6 (d, *J* = 2.4 Hz), 107.3 (d, *J* = 16.4 Hz), 97.8 (d, *J* = 28.2 Hz), 47.2, 25.8. HRMS (ESI) calcd for C₂₂H₁₆F₂N₄ (M + H)⁺: 375.1416, found 375.1417. LC-MS Purity: 96.2 %, R_t = 1.95 min.

6-fluoro-2-((7-fluoro-1H-indol-3-yl)methyl)-1-(pyridin-3-ylmethyl)-1H-benzo[d]imidazole (6) ¹H NMR (400 MHz, Methanol-*d*₄) δ 8.23 – 8.18 (m, 1H), 7.94 – 7.90 (m, 1H), 7.70 – 7.65 (m, 1H), 7.19 (d, *J* = 8.0 Hz, 1H), 7.10 – 7.02 (m, 3H), 6.99 – 6.93 (m, 1H), 6.89 – 6.82 (m, 2H), 6.75 (ddd, *J* = 11.4, 7.8 Hz, 1H), 5.47 (s, 2H), 4.48 (s, 2H). ¹³C NMR (101 MHz, Methanol-*d*₄) δ 161.2 (d, *J* = 239.2 Hz), 156.5 (d, *J* = 2.9 Hz), 151.0 (d, *J* = 243.5 Hz), 148.7, 147.7, 139.1 (d, *J* = 1.1 Hz), 137.0 (d, *J* = 13.2 Hz), 135.3, 133.3, 132.1 (d, *J* = 5.7 Hz), 126.0 (d, *J* = 13.7 Hz), 125.7, 124.5, 120.6 (d, *J* = 10.3 Hz), 120.5 (d, *J* = 6.4 Hz), 115.3 (d, *J* = 3.4 Hz), 111.8 (d, *J* = 25.3 Hz), 110.6 (d, *J* = 2.4 Hz), 107.3 (d, *J* = 16.3 Hz), 97.9 (d, *J* = 28.1 Hz), 45.9, 25.7. HRMS (ESI) calcd for C₂₂H₁₆F₂N₄ (M + H)⁺: 375.1416, found 375.1411. LC-MS Purity: 99.2 %, R_t = 2.27 min.

2-(6-fluoro-2-((7-fluoro-1H-indol-3-yl)methyl)-1H-benzo[d]imidazol-1-yl)ethan-1-ol (7) ¹H NMR (400 MHz, Methanol-*d*₄) δ 7.57 (dd, *J* = 8.8, 4.8 Hz, 1H), 7.30 – 7.22 (m, 2H), 7.17 – 7.13 (m, 1H), 7.04 – 6.97 (m, 1H), 6.93 – 6.87 (m, 1H), 6.85 – 6.78 (m, 1H), 4.50 (d, *J* = 1.0 Hz, 2H), 4.24 (t, *J* = 5.4 Hz, 2H), 3.67 (t, *J* = 5.4 Hz, 2H). HRMS (ESI) calcd for C₁₈H₁₅F₂N₃O (M + H)⁺: 328.1256, found 328.1265. LC-MS Purity: 96.9 %, R_t = 1.96 min.

6-fluoro-2-((7-fluoro-1H-indol-3-yl)methyl)-1-methyl-1H-benzo[d]imidazole (8) ¹H NMR (400 MHz, Chloroform-*d*) δ 8.41 (s, 1H), 7.67 (ddd, *J* = 8.7, 4.9, 0.5 Hz, 1H), 7.40 – 7.34 (m, 1H), 7.04 – 6.96 (m, 3H), 6.95 (ddd, *J* = 8.7, 2.5, 0.5 Hz, 1H), 6.93 – 6.87 (m, 1H), 4.40 (d, *J* = 1.1 Hz, 2H), 3.59 (s, 3H). HRMS (ESI) calcd for C₁₇H₁₃F₂N₃ (M + H)⁺: 298.1150, found 298.1152. LC-MS Purity: 96.8 %, R_t = 2.02 min.

6-fluoro-2-((7-fluoro-1H-indol-3-yl)methyl)-1-isobutyl-1H-benzo[d]imidazole (9) ¹H NMR (400 MHz, Chloroform-*d*) δ 8.50 (s, 1H), 7.66 (ddd, *J* = 8.2, 4.9, 1.0 Hz, 1H), 7.36 – 7.30 (m, 1H), 7.03 – 6.94 (m, 4H), 6.92 – 6.86 (m, 1H), 4.39 (d, *J* = 1.1 Hz, 2H), 3.79 (d, *J* = 7.7 Hz, 2H), 2.16 (m, 1H), 0.89 (d, *J* =

6.7 Hz, 6H). HRMS (ESI) calcd for $C_{20}H_{19}F_2N_3$ ($M + H$)⁺: 340.1620, found 340.1636. LC-MS Purity: 99.2 %, $R_t = 2.47$ min.

6-fluoro-2-((7-fluoro-1H-indol-3-yl)methyl)-1-neopentyl-1H-benzo[d]imidazole (10) ¹H NMR (400 MHz, DMSO-*d*₆) δ 11.43 (s, 1H), 7.52 (dd, $J = 8.7, 5.0$ Hz, 1H), 7.44 (dd, $J = 9.8, 2.5$ Hz, 1H), 7.36 (s, 1H), 7.31 – 7.25 (m, 1H), 7.00 – 6.93 (m, 1H), 6.92 – 6.84 (m, 2H), 4.36 (s, 2H), 4.05 (s, 2H), 1.00 (s, 9H). HRMS (ESI) calcd for $C_{21}H_{21}F_2N_3$ ($M + H$)⁺: 354.1776, found 354.1784. LC-MS Purity: 98.2 %, $R_t = 2.53$ min.

*6-fluoro-2-((7-fluoro-1H-indol-3-yl)methyl-*d*₂)-1H-benzo[d]imidazole (11)*. Compound **2** (145 mg, 0.51 mmol) was suspended in DMSO-*d*₆/D₂O (2.5 mL/7.5 mL). The reaction mixture was then heated at 160 °C by microwave for 5.0 h. After cooling to room temperature, the reaction mixture was then poured to 50 mL of ethyl acetate, washed by 50 mL of water three times. The organic phase was dried by Na₂SO₄, the solvent was then removed by rotavapor. The residue was then purified by silica gel flash column chromatography to yield 138 mg of compound **11** (95% yield).

*6-fluoro-2-((7-fluoro-1H-indol-3-yl)methyl-*d*₂)-1H-benzo[d]imidazole (11)* ¹H NMR (400 MHz, DMSO-*d*₆) δ 12.22 – 12.16 (m, 1H), 11.47 (s, 1H), 7.51 (m, 0.5 H), 7.39 – 7.28 (m, 3H), 7.16 (m, 0.5 H), 6.99 – 6.87 (m, 3H). HRMS (ESI) calcd for $C_{16}H_9D_2F_2N_3$ ($M + H$)⁺: 286.1119, found 286.1123. LC-MS Purity: 98.8 %, $R_t = 2.36$ min.

(5-fluoro-1H-indol-2-yl)(7-fluoro-1H-indol-3-yl)methanone (12). In a 250 mL flask with a magnetic stirring bar, 5-fluoroindole-2-carboxylic acid (1.0 g, 5.58 mmol), SOCl₂ (2.0 mL) and DMF (30 μ L) were dissolved in 30 mL of ethyl ether. The reaction mixture was stirred at room temperature for 4.0 h. After removing ethyl ether and SOCl₂ by rotavapor, the residue and 7-fluoroindole (905 mg, 6.7 mmol) were dissolved in 20 mL of DCM and 15 mL of nitromethane. To the reaction mixture, was added SnCl₄ (1N in DCM) (7.3 mL, 7.3 mmol) by syringe. The mixture was stirred at room temperature for overnight. After quenching by 150 mL of ice-water, the mixture was extracted by 150 mL of ethyl acetate. The organic phase was dried by Na₂SO₄, the solvent was removed by rotavapor. The residue was purified by silica gel column chromatography to yield 510 mg of compound **12** with a yield of 31%.

(5-fluoro-1H-indol-2-yl)(7-fluoro-1H-indol-3-yl)methanone (12) ¹H NMR (400 MHz, DMSO-*d*₆) δ 12.69 (s, 1H), 11.91 (s, 1H), 8.47 (s, 1H), 8.10 (d, $J = 8.0$ Hz, 1H), 7.52 – 7.48 (m, 1H), 7.47 – 7.43 (m, 1H), 7.38 (dd, $J = 2.3, 0.9$ Hz, 1H), 7.26 – 7.19 (m, 1H), 7.17 – 7.09 (m, 2H). ¹³C NMR (101 MHz, DMSO-*d*₆) δ 180.2 (d, $J = 1.2$ Hz), 157.2 (d, $J = 233.2$ Hz), 149.2 (d, $J = 244.8$ Hz), 137.5, 134.5, 134.0,

130.1 (d, $J = 4.9$ Hz), 127.3 (d, $J = 10.6$ Hz), 124.4 (d, $J = 13.4$ Hz), 122.4 (d, $J = 6.1$ Hz), 117.6 (d, $J = 3.5$ Hz), 115.8 (d, $J = 1.8$ Hz), 113.8 (d, $J = 9.6$ Hz), 113.4 (d, $J = 26.7$ Hz), 108.1 (d, $J = 15.6$ Hz), 107.6 (d, $J = 5.4$ Hz), 106.3 (d, $J = 22.8$ Hz). HRMS (ESI) calcd for $C_{17}H_{10}F_2N_2O$ ($M + Na$)⁺: 319.0653, found: 319.0666. LC-MS Purity: 98.2 %, $R_t = 2.73$ min.

General procedure for SeO_2 oxidation:

In a 100 mL flask with a magnetic stirring bar, compound **2** (1.2 g, 4.2 mmol) and SeO_2 (932 mg, 8.4 mmol) were suspended in 20 mL of 1,4-dioxane. The reaction mixture was then heated at 100 °C by oil bath for 4.0 h. After cooling to room temperature, the reaction mixture was then poured to 200 mL of ethyl acetate, washed by 100 mL of $NaHCO_3$ saturated aqueous solution three times. The organic phase was dried by Na_2SO_4 and the solvent was removed by rotavapor. The residue was then purified by silica gel column chromatography to yield 890 mg of compound **13** (71% yield).

(6-fluoro-1H-benzo[d]imidazol-2-yl)(7-fluoro-1H-indol-3-yl)methanone (**13**) ¹H NMR (400 MHz, $DMSO-d_6$) δ 13.47 (s, 0.5H), 13.44 (s, 0.5H), 12.85 (s, 1H), 9.34 (d, $J = 5.2$ Hz, 1H), 8.20 (d, $J = 7.9$ Hz, 1H), 7.91 (dd, $J = 8.9, 4.9$ Hz, 0.5H), 7.69 (dd, $J = 9.7, 2.5$ Hz, 0.5H), 7.60 (dd, $J = 8.9, 4.9$ Hz, 0.5H), 7.38 – 7.11 (m, 3.5H). ¹³C NMR (101 MHz, $DMSO-d_6$) δ 177.2, 161.3, 160.1, 158.9, 157.8, 150.7, 150.5, 150.2, 148.1, 143.4, 143.3, 139.8, 138.7, 138.6, 134.3, 134.2, 130.8, 130.1, 130.1, 124.2, 124.1, 123.2, 123.1, 122.3, 122.2, 117.7, 117.7, 114.5, 114.4, 113.7, 113.6, 113.5, 111.8, 111.6, 108.6, 108.4, 106.0, 105.7, 98.6, 98.3. HRMS (ESI) calcd for $C_{16}H_9F_2N_3O$ ($M + Na$)⁺: 320.0606, found: 320.0620. LC-MS Purity: 99.8 %, $R_t = 2.68$ min.

(1H-benzo[d]imidazol-2-yl)(1H-indol-3-yl)methanone (**14**) ¹H NMR (400 MHz, $DMSO-d_6$) δ 13.28 (s, 1H), 12.24 (s, 1H), 9.36 (d, $J = 3.2$ Hz, 1H), 8.42 – 8.37 (m, 1H), 7.86 (d, $J = 8.3$ Hz, 1H), 7.62 – 7.55 (m, 2H), 7.40 – 7.25 (m, 4H). HRMS (ESI) calcd for $C_{16}H_{11}N_3O$ ($M + H$)⁺: 262.0975, found 262.0978. LC-MS Purity: 99.2 %, $R_t = 2.46$ min.

(1H-benzo[d]imidazol-2-yl)(7-fluoro-1H-indol-3-yl)methanone (**15**) ¹H NMR (400 MHz, $DMSO-d_6$) δ 13.34 (s, 1H), 12.83 (s, 1H), 9.39 (d, $J = 3.2$ Hz, 1H), 8.22 (d, $J = 7.5$ Hz, 1H), 7.88 (d, $J = 8.1$ Hz, 1H), 7.61 (d, $J = 8.0$ Hz, 1H), 7.43 – 7.23 (m, 3H), 7.20 – 7.09 (m, 1H). HRMS (ESI) calcd for $C_{16}H_{10}FN_3O$ ($M + H$)⁺: 280.0881, found 280.0893. LC-MS Purity: 99.6 %, $R_t = 2.59$ min.

(6-fluoro-1H-benzo[d]imidazol-2-yl)(1H-indol-3-yl)methanone (**16**) ¹H NMR (400 MHz, $DMSO-d_6$) δ 13.39 (s, 1H), 12.26 (s, 1H), 9.32 (s, 1H), 8.44 – 8.35 (m, 1H), 7.88 (s, 0.5H), 7.75 – 7.51 (m, 2H), 7.37

– 7.17 (m, 3.5H). HRMS (ESI) calcd for $C_{16}H_{10}FN_3O$ ($M + H$)⁺: 280.0881, found 280.0886. LC-MS Purity: 99.6 %, $R_t = 2.53$ min.

Procedure for the preparation of 4-fluoro-*N*¹-methylbenzene-1,2-diamine and 6-fluoro-*N*¹-methylbenzene-1,2-diamine

tert-butyl (3-fluoro-2-nitrophenyl)carbamate

In a 100 mL flask with a magnetic stirring bar, 3-fluoro-2-nitroaniline (1.0 g, 6.41 mmol), Boc_2O (3.1 g, 14.1 mmol) and DMAP (200 mg) were dissolved in 20 mL of DMF. The reaction mixture was stirred overnight at room temperature and then diluted by 100 mL of ethyl acetate. The ethyl acetate solution was washed by 1N HCl (50 mL) three times, dried by Na_2SO_4 , and the solvent was removed by rotavapor. The residue was dissolved in 16 mL of DCM with 3.0 vol % TFA (0.5 mL, 9.6 mmol) (1.5 equiv). After stirring at room temperature for 2.0 h, the reaction mixture was diluted by 100 mL of ethyl acetate, washed by 50 mL of $NaHCO_3$ saturated aqueous solution three times. The organic phase was dried by Na_2SO_4 , the solvent was removed by rotavapor. The residue was purified by silica gel column chromatography to yield 1.58 g of *tert-butyl (3-fluoro-2-nitrophenyl)carbamate* (96 % yield).

The *tert-butyl (3-fluoro-2-(methylamino)phenyl)carbamate* was obtained by monomethylating of *tert-butyl (2-amino-3-fluorophenyl)carbamate* following procedures in literature.[66]

tert-butyl (5-fluoro-2-(methylamino)phenyl)carbamate

In a 100 mL flask with a magnetic stirring bar, *tert-butyl (2-amino-5-fluorophenyl)carbamate* (0.6 g, 2.65 mmol), CH_3I (376 mg, 2.65 mmol) and Na_2CO_3 (310 mg, 2.92 mmol) were suspended in 10 mL of DMF. The reaction mixture was stirred overnight at room temperature and then diluted by 100 mL of ethyl acetate. The ethyl acetate solution was washed by water (100 mL) three times, dried by Na_2SO_4 , the solvent was removed by rotavapor. The residue was purified by silica gel column chromatography to yield 255 mg of *tert-butyl (5-fluoro-2-(methylamino)phenyl)carbamate* with a yield of 40 %.

(4-fluoro-1H-benzo[d]imidazol-2-yl)(7-fluoro-1H-indol-3-yl)methanone (17) ¹H NMR (400 MHz, $DMSO-d_6$) δ 13.56 (s, 1H), 12.98 (s, 1H), 9.33 (s, 1H), 8.20 (d, $J = 7.9$ Hz, 1H), 7.61 – 7.40 (m, 1H), 7.32 (m, 2H), 7.15 (m, 2H). HRMS (ESI) calcd for $C_{16}H_9F_2N_3O$ ($M + H$)⁺: 298.0786, found 298.0794. LC-MS Purity: 99.8 %, $R_t = 2.71$ min.

(7-fluoro-1H-indol-3-yl)(1-methyl-1H-benzodimidazol-2-yl)methanone (**18**) ^1H NMR (500 MHz, DMSO- d_6) δ 12.78 (s, 1H), 8.97 (s, 1H), 8.20 (d, $J = 7.9$ Hz, 1H), 7.88 (d, $J = 8.1$ Hz, 1H), 7.75 (d, $J = 8.1$ Hz, 1H), 7.45 (ddd, $J = 8.1, 7.0, 1.1$ Hz, 1H), 7.37 (ddd, $J = 8.1, 7.1, 1.1$ Hz, 1H), 7.30 – 7.24 (m, 1H), 7.18 – 7.12 (m, 1H), 4.14 (s, 3H). HRMS (ESI) calcd for $\text{C}_{17}\text{H}_{12}\text{FN}_3\text{O}$ ($\text{M} + \text{H}$) $^+$: 294.1037, found 294.1048. LC-MS Purity: 99.3 %, $R_t = 2.68$ min.

(4-fluoro-1-methyl-1H-benzodimidazol-2-yl)(7-fluoro-1H-indol-3-yl)methanone (**19**) ^1H NMR (400 MHz, DMSO- d_6) δ 12.82 (s, 1H), 8.92 (s, 1H), 8.18 (d, $J = 7.9$ Hz, 1H), 7.59 (d, $J = 8.3$ Hz, 1H), 7.48 – 7.39 (m, 1H), 7.31 – 7.24 (m, 1H), 7.22 – 7.09 (m, 2H), 4.14 (s, 3H). HRMS (ESI) calcd for $\text{C}_{17}\text{H}_{11}\text{F}_2\text{N}_3\text{O}$ ($\text{M} + \text{H}$) $^+$: 312.0943, found 312.0956. LC-MS Purity: 99.6 %, $R_t = 2.80$ min.

(5-fluoro-1-methyl-1H-benzodimidazol-2-yl)(7-fluoro-1H-indol-3-yl)methanone (**20**) ^1H NMR (400 MHz, DMSO- d_6) δ 12.80 (s, 1H), 8.94 (d, $J = 2.2$ Hz, 1H), 8.18 (dd, $J = 7.9, 2.2$ Hz, 1H), 7.81 – 7.72 (m, 1H), 7.72 – 7.63 (m, 1H), 7.37 – 7.21 (m, 2H), 7.14 (ddd, $J = 10.6, 7.9, 2.2$ Hz, 1H), 4.13 (s, 3H). HRMS (ESI) calcd for $\text{C}_{17}\text{H}_{11}\text{F}_2\text{N}_3\text{O}$ ($\text{M} + \text{H}$) $^+$: 312.0943, found 312.0953. LC-MS Purity: 99.8 %, $R_t = 2.79$ min.

(6-fluoro-1-methyl-1H-benzodimidazol-2-yl)(7-fluoro-1H-indol-3-yl)methanone (**21**) ^1H NMR (400 MHz, DMSO- d_6) δ 12.77 (s, 1H), 8.93 (s, 1H), 8.17 (d, $J = 7.9$ Hz, 1H), 7.88 (dd, $J = 8.9, 5.0$ Hz, 1H), 7.61 (dd, $J = 9.4, 2.5$ Hz, 1H), 7.28 – 7.17 (m, 2H), 7.16 – 7.08 (m, 1H), 4.09 (s, 3H). ^{13}C NMR (101 MHz, DMSO- d_6) δ 179.1 (d, $J = 1.5$ Hz), 160.1 (d, $J = 239.8$ Hz), 149.2 (d, $J = 244.9$ Hz), 148.4 (d, $J = 3.1$ Hz), 139.0, 137.7, 136.7 (d, $J = 14.0$ Hz), 130.0 (d, $J = 4.7$ Hz), 124.1 (d, $J = 13.3$ Hz), 123.1 (d, $J = 6.1$ Hz), 122.2 (d, $J = 10.4$ Hz), 117.6 (d, $J = 3.4$ Hz), 115.5 (d, $J = 2.0$ Hz), 111.9 (d, $J = 25.7$ Hz), 108.4 (d, $J = 15.7$ Hz), 97.6 (d, $J = 27.9$ Hz), 32.4. HRMS (ESI) calcd for $\text{C}_{17}\text{H}_{11}\text{F}_2\text{N}_3\text{O}$ ($\text{M} + \text{Na}$) $^+$: 334.0762, found: 334.0765. LC-MS Purity: 96.3 %, $R_t = 2.78$ min.

(7-fluoro-1-methyl-1H-benzodimidazol-2-yl)(7-fluoro-1H-indol-3-yl)methanone (**22**) ^1H NMR (400 MHz, DMSO- d_6) δ 12.82 (s, 1H), 8.84 (d, $J = 2.5$ Hz, 1H), 8.17 (dd, $J = 8.0, 2.4$ Hz, 1H), 7.69 (dd, $J = 8.1, 2.4$ Hz, 1H), 7.34 – 7.19 (m, 3H), 7.19 – 7.08 (m, 1H), 4.25 (s, 3H). HRMS (ESI) calcd for $\text{C}_{17}\text{H}_{11}\text{F}_2\text{N}_3\text{O}$ ($\text{M} + \text{H}$) $^+$: 312.0943, found 312.0956. LC-MS Purity: 99.7 %, $R_t = 2.99$ min.

(6-fluoro-1-methyl-1H-benzodimidazol-2-yl)(1H-indol-3-yl)methanone (**23**) ^1H NMR (500 MHz, DMSO- d_6) δ 12.21 (s, 1H), 8.88 (s, 1H), 8.41 – 8.32 (m, 1H), 7.88 (dd, $J = 8.8, 4.9$ Hz, 1H), 7.66 (dd, $J = 9.4, 2.5$ Hz, 1H), 7.61 – 7.54 (m, 1H), 7.32 – 7.26 (m, 2H), 7.22 (ddd, $J = 9.9, 8.9, 2.5$ Hz, 1H), 4.10

(s, 3H). HRMS (ESI) calcd for $C_{17}H_{12}FN_3O$ ($M + H$)⁺: 294.1037, found 294.1051. LC-MS Purity: 99.2 %, $R_t = 2.71$ min.

(6-fluoro-1-methyl-1H-benzo[d]imidazol-2-yl)(4-fluoro-1H-indol-3-yl)methanone (**24**) ¹H NMR (500 MHz, DMSO-*d*₆) δ 12.42 (s, 1H), 8.67 (s, 1H), 7.85 (dd, $J = 8.9, 5.0$ Hz, 1H), 7.66 (dd, $J = 9.4, 2.5$ Hz, 1H), 7.39 (d, $J = 8.1$ Hz, 1H), 7.30 – 7.25 (m, 1H), 7.21 (ddd, $J = 9.8, 8.8, 2.5$ Hz, 1H), 7.00 (dd, $J = 11.1, 7.8$ Hz, 1H), 4.05 (s, 3H). HRMS (ESI) calcd for $C_{17}H_{11}F_2N_3O$ ($M + H$)⁺: 312.0943, found 312.0954. LC-MS Purity: 99.2 %, $R_t = 2.59$ min.

(6-fluoro-1-methyl-1H-benzo[d]imidazol-2-yl)(5-fluoro-1H-indol-3-yl)methanone (**25**) ¹H NMR (500 MHz, DMSO-*d*₆) δ 12.31 (s, 1H), 8.96 (s, 1H), 8.04 (dd, $J = 9.9, 2.6$ Hz, 1H), 7.88 (dd, $J = 8.9, 5.0$ Hz, 1H), 7.67 (dd, $J = 9.4, 2.5$ Hz, 1H), 7.59 (dd, $J = 8.8, 4.6$ Hz, 1H), 7.23 (ddd, $J = 9.8, 8.9, 2.5$ Hz, 1H), 7.19 – 7.10 (m, 1H), 4.11 (s, 3H). HRMS (ESI) calcd for $C_{17}H_{11}F_2N_3O$ ($M + H$)⁺: 312.0943, found 312.0956. LC-MS Purity: 95.8 %, $R_t = 2.92$ min.

(6-fluoro-1-methyl-1H-benzo[d]imidazol-2-yl)(6-fluoro-1H-indol-3-yl)methanone (**26**) ¹H NMR (500 MHz, DMSO-*d*₆) δ 12.23 (s, 1H), 8.90 (s, 1H), 8.34 (dd, $J = 8.7, 5.6$ Hz, 1H), 7.88 (dd, $J = 8.9, 4.9$ Hz, 1H), 7.66 (dd, $J = 9.4, 2.5$ Hz, 1H), 7.37 (dd, $J = 9.6, 2.4$ Hz, 1H), 7.22 (ddd, $J = 9.8, 8.8, 2.5$ Hz, 1H), 7.14 (ddd, $J = 9.8, 8.7, 2.4$ Hz, 1H), 4.10 (s, 3H). HRMS (ESI) calcd for $C_{17}H_{11}F_2N_3O$ ($M + H$)⁺: 312.0943, found 312.0955. LC-MS Purity: 99.7 %, $R_t = 2.87$ min.

(6-fluoro-1-methyl-1H-benzo[d]imidazol-2-yl)(7-fluoro-1-methyl-1H-indol-3-yl)methanone (**27**) ¹H NMR (400 MHz, DMSO-*d*₆) δ 8.87 (s, 1H), 8.20 (dd, $J = 8.0, 0.9$ Hz, 1H), 7.88 (dd, $J = 8.9, 4.9$ Hz, 1H), 7.67 (dd, $J = 9.4, 2.5$ Hz, 1H), 7.31 – 7.20 (m, 2H), 7.15 (ddd, $J = 12.6, 7.9, 0.9$ Hz, 1H), 4.11 (d, $J = 2.3$ Hz, 3H), 4.09 (s, 3H). HRMS (ESI) calcd for $C_{18}H_{13}F_2N_3O$ ($M + H$)⁺: 326.1099, found 326.1113. LC-MS Purity: 99.1 %, $R_t = 3.03$ min.

General procedure for the preparation of compounds **28**, **30** and **31**

In a 25 mL flask with a magnetic stirring bar, compound **21** (200 mg, 0.64 mmol), 1-bromo-2-chloroethane (368 mg, 2.56 mmol) and K_2CO_3 (353 mg, 2.56 mmol) were suspended in 10 mL of acetone. After sealing by rubber stopper, the flask was heated at 70 °C in an oil bath for 3 h. Then the reaction mixture was diluted by 100 mL of ethyl acetate. The ethyl acetate solution was washed by water (50 mL) three times, dried by Na_2SO_4 , the solvent was removed by rotavapor. The residue was purified by silica gel column chromatography to yield 203 mg of white solid with a yield of 85 %.

In a 10 mL flask with a magnetic stirring bar, the intermediate prepared above (203 mg, 0.54 mmol), TBAI (40 mg, 0.11 mmol) were dissolved in 3 mL of morpholine. After sealing by a rubber stopper, the flask was heated at 100 °C in an oil bath for 4 h, and then diluted by 50 mL of ethyl acetate. The ethyl acetate solution was washed by water (50 mL) three times, dried by Na₂SO₄, the solvent was removed by rotavapor. The residue was purified by silica gel column chromatography to yield compound **28** (183 mg, 80% yield).

(7-fluoro-1-(2-morpholinoethyl)-1H-indol-3-yl)(6-fluoro-1-methyl-1H-benzo[d]imidazol-2-yl)methanone (28) ¹H NMR (400 MHz, DMSO-*d*₆) δ 9.02 (s, 1H), 8.22 (d, *J* = 8.0 Hz, 1H), 7.87 – 7.80 (m, 1H), 7.68 (dd, *J* = 9.4, 2.5 Hz, 1H), 7.30 – 7.21 (m, 2H), 7.19 – 7.11 (m, 1H), 4.54 (t, *J* = 6.1 Hz, 2H), 4.10 (s, 3H), 3.59 (t, *J* = 4.4 Hz, 4H), 2.74 (t, *J* = 6.1 Hz, 2H), 2.47 (t, *J* = 4.4 Hz, 4H). ¹³C NMR (101 MHz, DMSO-*d*₆) δ 178.8, 160.1 (d, *J* = 239.6 Hz), 149.4 (d, *J* = 244.3 Hz), 148.5 (d, *J* = 3.1 Hz), 143.5, 137.8, 136.8 (d, *J* = 13.9 Hz), 130.8 (d, *J* = 4.1 Hz), 123.7 (d, *J* = 9.3 Hz), 123.4 (d, *J* = 6.6 Hz), 122.0 (d, *J* = 10.5 Hz), 117.9 (d, *J* = 3.6 Hz), 114.2, 111.9 (d, *J* = 25.9 Hz), 109.3 (d, *J* = 17.9 Hz), 97.8 (d, *J* = 27.8 Hz), 66.2, 57.8, 53.2, 46.1 (d, *J* = 5.0 Hz), 32.4. HRMS (ESI) calcd for C₂₃H₂₂F₂N₄O₂ (M + H)⁺: 425.1784, found: 425.1799. LC-MS Purity: 99.2 %, R_t = 2.43 min.

(6-fluoro-1-(2-morpholinoethyl)-1H-benzo[d]imidazol-2-yl)(7-fluoro-1H-indol-3-yl)methanone (29) ¹H NMR (400 MHz, DMSO-*d*₆) δ 12.82 (s, 1H), 8.82 (s, 1H), 8.15 (d, *J* = 7.9 Hz, 1H), 7.88 (dd, *J* = 8.9, 4.9 Hz, 1H), 7.68 (dd, *J* = 9.4, 2.5 Hz, 1H), 7.29 – 7.18 (m, 2H), 7.14 (dd, *J* = 11.3, 7.9 Hz, 1H), 4.74 (t, *J* = 5.9 Hz, 2H), 3.17 (t, *J* = 4.6 Hz, 4H), 2.58 (t, *J* = 5.9 Hz, 2H), 2.31 (t, *J* = 4.5 Hz, 4H). HRMS (ESI) calcd for C₂₂H₂₀F₂N₄O₂ (M + H)⁺: 411.1627, found 411.1627. LC-MS Purity: 99.3 %, R_t = 2.28 min.

(7-fluoro-1-(3-morpholinopropyl)-1H-indol-3-yl)(6-fluoro-1-methyl-1H-benzo[d]imidazol-2-yl)methanone (30) ¹H NMR (400 MHz, DMSO-*d*₆) δ 8.93 (s, 1H), 8.23 (dd, *J* = 7.9, 2.8 Hz, 1H), 7.88 – 7.78 (m, 1H), 7.65 (dd, *J* = 9.4, 2.6 Hz, 1H), 7.31 – 7.20 (m, 2H), 7.19 – 7.11 (m, 1H), 4.47 (t, *J* = 6.6 Hz, 2H), 4.08 (s, 3H), 3.53 (t, *J* = 4.4 Hz, 4H), 2.30 (t, *J* = 4.4 Hz, 4H), 2.22 (t, *J* = 6.3 Hz, 2H), 2.02 – 1.92 (m, 2H). HRMS (ESI) calcd for C₂₄H₂₄F₂N₄O₂ (M + H)⁺: 439.1940, found 439.1942. LC-MS Purity: 98.6 %, R_t = 2.35 min.

(7-fluoro-1-(4-morpholinobutyl)-1H-indol-3-yl)(6-fluoro-1-methyl-1H-benzo[d]imidazol-2-yl)methanone (31) ¹H NMR (400 MHz, DMSO-*d*₆) δ 8.92 (s, 1H), 8.22 (d, *J* = 8.0 Hz, 1H), 7.92 – 7.80 (m, 1H), 7.66 (dd, *J* = 9.4, 2.5 Hz, 1H), 7.32 – 7.20 (m, 2H), 7.16 (dd, *J* = 12.7, 8.0 Hz, 1H), 4.44 (t, *J* =

7.2 Hz, 2H), 4.09 (s, 3H), 3.49 (t, $J = 4.5$ Hz, 4H), 2.37 – 2.16 (m, 6H), 1.85 (p, $J = 7.4$ Hz, 2H), 1.44 (p, $J = 7.3$ Hz, 2H). HRMS (ESI) calcd for $C_{25}H_{26}F_2N_4O_2$ ($M + H$)⁺: 453.2097, found 453.2102. LC-MS Purity: 99.6 %, $R_t = 2.50$ min.

(*1-butyl-7-fluoro-1H-indol-3-yl*)(*6-fluoro-1-methyl-1H-benzo[d]imidazol-2-yl*)methanone (**32**) ¹H NMR (500 MHz, Chloroform-*d*) δ 8.83 (s, 1H), 8.34 (d, $J = 8.0$ Hz, 1H), 7.83 (dd, $J = 9.5, 4.8$ Hz, 1H), 7.28 – 7.20 (m, 1H), 7.16 – 7.07 (m, 2H), 7.00 (dd, $J = 12.5, 7.9$ Hz, 1H), 4.36 (t, $J = 7.3$ Hz, 2H), 4.14 (s, 3H), 1.91 (p, $J = 7.3$ Hz, 2H), 1.46 – 1.34 (m, 2H), 0.96 (t, $J = 7.4$ Hz, 3H). ¹³C NMR (126 MHz, Chloroform-*d*) δ 179.3, 161.1 (d, $J = 243.0$ Hz), 145.0 (d, $J = 245.3$ Hz), 148.8 (d, $J = 3.2$ Hz), 141.6, 138.3, 137.0 (d, $J = 13.3$ Hz), 131.6 (d, $J = 4.1$ Hz), 124.4 (d, $J = 9.7$ Hz), 123.6 (d, $J = 6.5$ Hz), 122.6 (d, $J = 10.3$ Hz), 118.5 (d, $J = 3.8$ Hz), 115.4 (d, $J = 1.4$ Hz), 112.4 (d, $J = 25.7$ Hz), 109.6 (d, $J = 18.0$ Hz), 96.7 (d, $J = 27.4$ Hz), 50.1 (d, $J = 5.0$ Hz), 33.3 (d, $J = 2.2$ Hz), 32.6, 20.0, 13.7. HRMS (ESI) calcd for $C_{21}H_{19}F_2N_3O$ ($M + Na$)⁺: 390.1388, found: 390.1404. LC-MS Purity: 99.5 %, $R_t = 3.19$ min.

General procedure for the preparation of compounds **33** and **34**

In a 25 mL flask with a magnetic stirring bar, compound **21** (200 mg, 0.64 mmol) was suspended in 6 mL of DMF. After cooling to 0 °C by an ice-water bath, NaH (65 wt %) (29 mg, 0.77 mmol) was added to the reaction mixture. After stirring at 0 °C for 1.0 h, ClSO₂CH₂CH₂Cl (157 mg, 0.96 mmol) was added. The reaction mixture was stirred overnight. The reaction mixture was diluted by 60 mL of ethyl acetate solution, and then washed by water (50 mL) three times, dried by Na₂SO₄, the solvent was removed by rotavapor. The residue was purified by silica gel column chromatography to yield 195 mg of white solid with a yield of 70 %.

In a 10 mL flask with a magnetic stirring bar, the intermediate prepared above (150 mg, 0.34 mmol), morpholine (296 mg, 3.4 mmol) and TBAI (26 mg, 0.07 mmol) were dissolved in 3 mL of DMSO and stirred at 110 °C for 6 h. After cooling to room temperature, it was diluted by 60 mL of ethyl acetate. The ethyl acetate solution was washed by water (60 mL) three times, dried by Na₂SO₄. The solvent was removed by rotavapor. The residue was purified by silica gel column chromatography to yield 116 mg of compound **33** (70 % yield).

(*7-fluoro-1-((2-morpholinoethyl)sulfonyl)-1H-indol-3-yl*)(*6-fluoro-1-methyl-1H-benzo[d]imidazol-2-yl*)methanone (**33**) ¹H NMR (500 MHz, Chloroform-*d*) δ 8.94 (s, 1H), 8.35 (d, $J = 8.0$ Hz, 1H), 7.85 (dd, $J = 9.5, 4.8$ Hz, 1H), 7.31 – 7.26 (m, 1H), 7.16 – 7.11 (m, 2H), 7.06 (dd, $J = 12.7, 8.0$ Hz, 1H), 4.83 (t, J

= 7.3 Hz, 2H), 4.16 (s, 3H), 3.68 – 3.63 (m, 4H), 3.52 (t, $J = 7.3$ Hz, 2H), 3.26 – 3.21 (m, 4H). HRMS (ESI) calcd for $C_{23}H_{22}F_2N_4O_4S$ ($M + H$)⁺: 489.1403, found: 489.1417. LC-MS Purity: 95.9 %, $R_t = 2.84$ min.

(7-fluoro-1-((2-(piperazin-1-yl)ethyl)sulfonyl)-1H-indol-3-yl)(6-fluoro-1-methyl-1H-benzo[d]imidazol-2-yl)methanone (**34**) ¹H NMR (500 MHz, Chloroform-*d*) δ 8.89 (s, 1H), 8.30 (d, $J = 7.9$ Hz, 1H), 7.86 – 7.79 (m, 1H), 7.26 – 7.21 (m, 1H), 7.13 – 7.07 (m, 2H), 7.02 (dd, $J = 12.5, 7.9$ Hz, 1H), 4.79 (t, $J = 7.3$ Hz, 2H), 4.12 (s, 3H), 3.49 (t, $J = 7.3$ Hz, 2H), 3.26 (t, $J = 4.8$ Hz, 4H), 2.89 (t, $J = 4.8$ Hz, 4H). HRMS (ESI) calcd for $C_{23}H_{23}F_2N_5O_3S$ ($M + H$)⁺: 488.1538, found 488.1564. LC-MS Purity: 97.5 %, $R_t = 2.50$ min.

Cell Culture and Bioactivity Test: HepG2 cells were cultured in low-glucose DMEM media supplemented with 10% FBS, 1% Penicillin/Streptomycin, 1% non-essential amino acid, 1% sodium pyruvate and 1% L-glutamine. When the cells reach 90% confluence, they were harvested and plated 1×10^5 cells per well in 96-well plate. After overnight settle-down, the culture medium was removed. 200 μ L of dose medium containing compounds or vehicle was added to each well. After 24 h, each well was refreshed with the same medium, followed by another 24 h incubation. Finally, medium was collected after centrifugation at 3000 rpm for 3 min and was used for ELISA.

ELISA Assay: ELISA assay was used to measure PCSK9 concentration in cell culture medium according to manufacture protocol (R&D system, DY3888). 100 μ L of 2.0 μ g/mL PCSK9 capture antibody in PBS was add into high-binding plate (R&D system, DY990). After overnight incubation at room temperature, the solution was removed and washed with ~ 400 μ L of washing buffer (0.05% Tween-20 in PBS) three times. Reagent diluent (300 μ L, 1% BSA in PBS) was added to each well and incubated for at least 1 h. Each of following steps was performed after the removal of previous solution and washing out remaining solution with washing buffer. PCSK9 standard or sample (100 μ L) with or without dilution in reagent was added to each well followed with 2 h incubation. Next, 100 μ L of 100 ng/mL PCSK9 detection antibody in reagent was added to each well followed with 2 h incubation. After detection antibody incubation, 100 μ L of Streptavidin-HRP was added to each well and incubated for 20 min. Finally, 100 μ L of TMB solution was added and incubated for 20 min followed with the addition of 50 μ L of stop solution (2 N H_2SO_4). After mixing, the optical density of each well was determined immediately using a microplate reader set to 450 nm and wavelength correction to 540 nm or 570 nm.

Subtract readings at 540 nm or 570 nm from the readings at 450 nm. Standard curve was generated by four parameters logistic (4-PL) curve-fit and used to measure the PCSK9 concentration in samples.

Statistical Analysis: All statistical analysis was done by GraphPad Prism. Statistical significance was analyzed by performing one-way ANOVA analysis of variance. Multiple group comparisons with vehicle or compound-treated group were followed Dunnett correction. Not significant (ns) $p > 0.05$, $*p \leq 0.05$, $**p \leq 0.01$, $***p \leq 0.001$, $****p \leq 0.0001$.

Pharmacokinetic Study: The animal studies were conducted following protocol A00582 (Attie) approved by the Institutional Animal Care and Use Committee (IACUC). The pharmacokinetic study of compound **12** and **13** were carried out with female BTBR mice. 2.0 mM of compound was suspended in DMSO (10 %) and Tween 80 (10%) in PBS (80%). A single dose of 6 mg/kg was administered by intraperitoneal injection (n = 3 mice), followed by blood collection via retro-orbital bleeding at 0.25, 0.5, 2.0, 4.0, 6.0 h.

Whole blood samples were added to a tube containing EDTA and centrifuged. Plasma was collected and stored at -20 °C. Compound standards were prepared with pooled plasma samples. 50 μ L of thawed plasma and standards were added into wells of Ostro Pass-Through Sample Preparation Plate (96-well) (Waters, Part Number 186005518) for solid-phase extraction. Acetonitrile (150 μ L, 1% formic acid) containing internal standard was added and mixed by pipette. Next, clear sample solution was eluted by positive pressure processor under 60 psi for 5 min. The sample solution can be used directly for LC-MS/MS analysis. In our case, we used QTrap-5500 and Acquity UPLC system to analyze the content of compound. MS data was analyzed by Analyst® software and standard curve was processed by four-parameter logistic (4-PL) curve-fit.

Hepatic Microsome Stability Assay: Metabolic stability was assessed in the presence of Human, mouse, and rat liver microsomes (XenoTech) at Sanford Burnham Prebys Medical Discovery Institute (SBP). All liquid dispenses and transfer steps were performed with the Freedom Evo automated liquid handler (Tecan US). NADPH, a required cofactor for CYP450 metabolism, was provided by the NADPH Regenerating System, Solutions A (BD Biosciences) and B (BD Biosciences). Compound stock solutions were initially prepared in 100% DMSO and subsequently diluted in acetonitrile for the assay. The pH of the reactions was kept at ~ 7.4 with potassium phosphate buffer (BD Biosciences). The reaction wells were prepared by adding microsomes to a well and allowed to warm to 37 °C. Then

compound was added to each well. The reactions were started by adding NADPH to the reaction well containing microsomes and compounds. Negative controls received buffer only (instead of NADPH). Immediately after reactions started, 0 min aliquots were promptly collected and mixed in a separate well with ice cold acetonitrile (spiked with internal standards) to quench the reactions. The remainder of the reaction volume was incubated at 37 °C with shaking. An additional aliquot was collected at 60 min after the start of the reaction and promptly quenched with ice cold acetonitrile (spiked with an internal standard). Samples were vortexed and centrifuged at 3700 rpm for 10 min. The amount of compound in the supernatant was determined by LC/MS/MS (ThermoScientific, Endura) and the percent of parent compound remaining after 60 min was calculated by the following formula:

$$CL_{\text{int}} \text{ (intrinsic clearance) } (\mu\text{L}/\text{min}/\text{mg}) = 0.693/(T_{1/2} [\text{microsomal protein}])$$

$$T_{1/2} \text{ (half-life)(min) } = 0.693/-k$$

$$k = \text{slope}$$

All reactions were run in triplicate, except negative controls (no NADPH) which were performed as single reactions. Results reported are the mean of each reaction triplicate, normalized to the internal standard, and expressed as the percent of compound remaining after the incubation time.

Acknowledgements

We thank NIH (R01GM120357) and the University of Wisconsin-Madison for financial support. We thank UW-Medicinal Chemistry Center (MCC) and Analytic Instrument Center (AIC) for instrumentation.

Abbreviations

PCSK9, Proprotein convertase subtilisin/kexin type 9; LDLR, Low-Density Lipoprotein Receptor; LDL-C, Low-density lipoprotein cholesterol; DIM, diindolylmethane; SAR, structure–activity relationship; EGF-A, epidermal growth factor precursor homology domain A; DFDIM, difluoro-2,3'-diindolylmethane; DFBIIM, difluorobenzoimidazolylindolylmethane; DFDIK, difluorodiindolylketone; DFBIK, difluorobenzoimidazolylindolylketone; CVD, Cardiovascular disease; ELISA, enzyme-linked immunosorbent assay; mAb, Monoclonal antibodies; RNAi, RNA interference; HSPG, heparan sulfate

proteoglycans; BBR, Berberine; MoA, mechanism of action; ADME, absorption, distribution, metabolism, and excretion; DCM, Dichloromethane, DMSO, Dimethyl sulfoxide; DMF, Dimethylformamide; DIPEA, *N,N*-Diisopropylethylamine; AcOH, Acetic acid; EDCI, *N*-(3-Dimethylaminopropyl)-*N'*-ethylcarbodiimide hydrochloride; HOBt, Hydroxybenzotriazole; DMAP, 4-Dimethylaminopyridine; TFA, Trifluoroacetic acid; TBAI, Tetrabutylammonium iodide; TLC, Thin-layer chromatography; UPLC, Ultra performance liquid chromatography; HRMS, High resolution mass spectrometry; EDTA, Ethylenediaminetetraacetic acid; PBS, Phosphate-Buffered Saline; DMEM, Dulbecco's Modified Eagle Medium; FBS, Fetal Bovine Serum; TMB, 3,3',5,5'-Tetramethylbenzidine; NADPH, Nicotinamide adenine dinucleotide phosphate; BSA, Bovine serum albumin; HRP, Horseradish peroxidase; FBS, fetal bovine serum.

Reference

- [1] M. Abifadel, M. Varret, J.-P. Rabès, D. Allard, K. Ouguerram, M. Devillers, C. Cruaud, S. Benjannet, L. Wickham, D. Erlich, A. Derré, L. Villéger, M. Farnier, I. Beucler, E. Bruckert, J. Chambaz, B. Chanu, J.-M. Lecerf, G. Luc, P. Moulin, J. Weissenbach, A. Prat, M. Krempf, C. Junien, N.G. Seidah, C. Boileau, Mutations in PCSK9 cause autosomal dominant hypercholesterolemia, *Nat. Genet.* 34 (2003) 154–156. <https://doi.org/10.1038/ng1161>.
- [2] N.G. Seidah, S. Benjannet, L. Wickham, J. Marcinkiewicz, S.B. Jasmin, S. Stifani, A. Basak, A. Prat, M. Chrétien, The secretory proprotein convertase neural apoptosis-regulated convertase 1 (NARC-1): Liver regeneration and neuronal differentiation, *Proc. Natl. Acad. Sci.* 100 (2003) 928–933. <https://doi.org/10.1073/pnas.0335507100>.
- [3] J.G. Robinson, M. Farnier, M. Krempf, J. Bergeron, G. Luc, M. Averna, E.S. Stroes, G. Langslet, F.J. Raal, M. El Shahawy, M.J. Koren, N.E. Lepor, C. Lorenzato, R. Pordy, U. Chaudhari, J.J.P. Kastelein, Efficacy and Safety of Alirocumab in Reducing Lipids and Cardiovascular Events, *N. Engl. J. Med.* 372 (2015) 1489–1499. <https://doi.org/10.1056/NEJMoa1501031>.
- [4] M.S. Sabatine, R.P. Giugliano, A.C. Keech, N. Honarpour, S.D. Wiviott, S.A. Murphy, J.F. Kuder, H. Wang, T. Liu, S.M. Wasserman, P.S. Sever, T.R. Pedersen, Evolocumab and Clinical Outcomes in Patients with Cardiovascular Disease, *N. Engl. J. Med.* 376 (2017) 1713–1722. <https://doi.org/10.1056/NEJMoa1615664>.

- [5] H.J. Kwon, T.A. Lagace, M.C. McNutt, J.D. Horton, J. Deisenhofer, Molecular basis for LDL receptor recognition by PCSK9, *Proc. Natl. Acad. Sci.* 105 (2008) 1820–1825. <https://doi.org/10.1073/pnas.0712064105>.
- [6] L. Shan, L. Pang, R. Zhang, N.J. Murgolo, H. Lan, J.A. Hedrick, PCSK9 binds to multiple receptors and can be functionally inhibited by an EGF-A peptide, *Biochem. Biophys. Res. Commun.* 375 (2008) 69–73. <https://doi.org/10.1016/j.bbrc.2008.07.106>.
- [7] Y. Zhang, C. Eigenbrot, L. Zhou, S. Shia, W. Li, C. Quan, J. Tom, P. Moran, P.D. Lello, N.J. Skelton, M. Kong-Beltran, A. Peterson, D. Kirchhofer, Identification of a Small Peptide That Inhibits PCSK9 Protein Binding to the Low Density Lipoprotein Receptor, *J. Biol. Chem.* 289 (2014) 942–955. <https://doi.org/10.1074/jbc.M113.514067>.
- [8] Y. Zhang, M. Ultsch, N.J. Skelton, D.J. Burdick, M.H. Beresini, W. Li, M. Kong-Beltran, A. Peterson, J. Quinn, C. Chiu, Y. Wu, S. Shia, P. Moran, P. Di Lello, C. Eigenbrot, D. Kirchhofer, Discovery of a cryptic peptide-binding site on PCSK9 and design of antagonists, *Nat. Struct. Mol. Biol.* 24 (2017) 848–856. <https://doi.org/10.1038/nsmb.3453>.
- [9] C.I. Schroeder, J.E. Swedberg, J.M. Withka, K.J. Rosengren, M. Akcan, D.J. Clayton, N.L. Daly, O. Cheneval, K.A. Borzilleri, M. Griffor, I. Stock, B. Colless, P. Walsh, P. Sunderland, A. Reyes, R. Dullea, M. Ammirati, S. Liu, K.F. McClure, M. Tu, S.K. Bhattacharya, S. Liras, D.A. Price, D.J. Craik, Design and Synthesis of Truncated EGF-A Peptides that Restore LDL-R Recycling in the Presence of PCSK9 In Vitro, *Chem. Biol.* 21 (2014) 284–294. <https://doi.org/10.1016/j.chembiol.2013.11.014>.
- [10] C. Lammi, C. Zaroni, G. Aiello, A. Arnoldi, G. Grazioso, Lupin Peptides Modulate the Protein-Protein Interaction of PCSK9 with the Low Density Lipoprotein Receptor in HepG2 Cells, *Sci. Rep.* 6 (2016) 1–13. <https://doi.org/10.1038/srep29931>.
- [11] C. Lammi, J. Sgrignani, A. Arnoldi, G. Grazioso, Biological Characterization of Computationally Designed Analogs of peptide TVFTSWEEYLDWV (Pep2-8) with Increased PCSK9 Antagonistic Activity, *Sci. Rep.* 9 (2019) 1–11. <https://doi.org/10.1038/s41598-018-35819-0>.
- [12] C. Lammi, J. Sgrignani, G. Roda, A. Arnoldi, G. Grazioso, Inhibition of PCSK9D374Y/LDLR Protein–Protein Interaction by Computationally Designed T9 Lupin Peptide, *ACS Med. Chem. Lett.* 10 (2019) 425–430. <https://doi.org/10.1021/acsmchemlett.8b00464>.

- [13] D.J. Burdick, N.J. Skelton, M. Ultsch, M.H. Beresini, C. Eigenbrot, W. Li, Y. Zhang, H. Nguyen, M. Kong-Beltran, J.G. Quinn, D. Kirchhofer, Design of Organo-Peptides As Bipartite PCSK9 Antagonists, *ACS Chem. Biol.* 15 (2020) 425–436. <https://doi.org/10.1021/acscchembio.9b00899>.
- [14] M.J. Graham, K.M. Lemonidis, C.P. Whipple, A. Subramaniam, B.P. Monia, S.T. Crooke, R.M. Crooke, Antisense inhibition of proprotein convertase subtilisin/kexin type 9 reduces serum LDL in hyperlipidemic mice, *J. Lipid Res.* 48 (2007) 763–767. <https://doi.org/10.1194/jlr.C600025-JLR200>.
- [15] N. Gupta, N. Fisker, M.-C. Asselin, M. Lindholm, C. Rosenbohm, H. Ørum, J. Elmén, N.G. Seidah, E.M. Straarup, A Locked Nucleic Acid Antisense Oligonucleotide (LNA) Silences PCSK9 and Enhances LDLR Expression In Vitro and In Vivo, *PLOS ONE*. 5 (2010) e10682. <https://doi.org/10.1371/journal.pone.0010682>.
- [16] M.W. Lindholm, J. Elmén, N. Fisker, H.F. Hansen, R. Persson, M.R. Møller, C. Rosenbohm, H. Ørum, E.M. Straarup, T. Koch, PCSK9 LNA Antisense Oligonucleotides Induce Sustained Reduction of LDL Cholesterol in Nonhuman Primates, *Mol. Ther.* 20 (2012) 376–381. <https://doi.org/10.1038/mt.2011.260>.
- [17] M.E. Visser, J.L. Witztum, E.S.G. Stroes, J.J.P. Kastelein, Antisense oligonucleotides for the treatment of dyslipidaemia, *Eur. Heart J.* 33 (2012) 1451–1458. <https://doi.org/10.1093/eurheartj/ehs084>.
- [18] E.P. van Poelgeest, M.R. Hodges, M. Moerland, Y. Tessier, A.A. Levin, R. Persson, M.W. Lindholm, K.D. Erichsen, H. Ørum, A.F. Cohen, J. Burggraaf, Antisense-mediated reduction of proprotein convertase subtilisin/kexin type 9 (PCSK9): a first-in-human randomized, placebo-controlled trial, *Br. J. Clin. Pharmacol.* 80 (2015) 1350–1361. <https://doi.org/10.1111/bcp.12738>.
- [19] K. Fitzgerald, S. White, A. Borodovsky, B.R. Bettencourt, A. Strahs, V. Clausen, P. Wijngaard, J.D. Horton, J. Taubel, A. Brooks, C. Fernando, R.S. Kauffman, D. Kallend, A. Vaishnav, A. Simon, A Highly Durable RNAi Therapeutic Inhibitor of PCSK9, *N. Engl. J. Med.* 376 (2017) 41–51. <https://doi.org/10.1056/NEJMoa1609243>.
- [20] K.K. Ray, U. Landmesser, L.A. Leiter, D. Kallend, R. Dufour, M. Karakas, T. Hall, R.P.T. Troquay, T. Turner, F.L.J. Visseren, P. Wijngaard, R.S. Wright, J.J.P. Kastelein, Inclisiran in Patients at High Cardiovascular Risk with Elevated LDL Cholesterol, *N. Engl. J. Med.* 376 (2017) 1430–1440. <https://doi.org/10.1056/NEJMoa1615758>.

- [21] A. Mullard, PCSK9-lowering RNAi contender clears first phase III trial, *Nat. Rev. Drug Discov.* 18 (2019) 737–737. <https://doi.org/10.1038/d41573-019-00153-1>.
- [22] S. Xu, S. Luo, Z. Zhu, J. Xu, Small molecules as inhibitors of PCSK9: Current status and future challenges, *Eur. J. Med. Chem.* 162 (2019) 212–233. <https://doi.org/10.1016/j.ejmech.2018.11.011>.
- [23] D. Pettersen, O. Fjellström, Small molecule modulators of PCSK9 – A literature and patent overview, *Bioorg. Med. Chem. Lett.* 28 (2018) 1155–1160. <https://doi.org/10.1016/j.bmcl.2018.02.046>.
- [24] J. Eder, R. Sedrani, C. Wiesmann, The discovery of first-in-class drugs: origins and evolution, *Nat. Rev. Drug Discov.* 13 (2014) 577–587. <https://doi.org/10.1038/nrd4336>.
- [25] D.C. Swinney, J. Anthony, How were new medicines discovered?, *Nat. Rev. Drug Discov.* 10 (2011) 507–519. <https://doi.org/10.1038/nrd3480>.
- [26] J.G. Moffat, F. Vincent, J.A. Lee, J. Eder, M. Prunotto, Opportunities and challenges in phenotypic drug discovery: an industry perspective, *Nat. Rev. Drug Discov.* 16 (2017) 531–543. <https://doi.org/10.1038/nrd.2017.111>.
- [27] W. Zheng, N. Thorne, J.C. McKew, Phenotypic screens as a renewed approach for drug discovery, *Drug Discov. Today*. 18 (2013) 1067–1073. <https://doi.org/10.1016/j.drudis.2013.07.001>.
- [28] K. Andries, P. Verhasselt, J. Guillemont, H.W.H. Göhlmann, J.-M. Neefs, H. Winkler, J.V. Gestel, P. Timmerman, M. Zhu, E. Lee, P. Williams, D. de Chaffoy, E. Huitric, S. Hoffner, E. Cambau, C. Truffot-Pernot, N. Lounis, V. Jarlier, A Diarylquinoline Drug Active on the ATP Synthase of *Mycobacterium tuberculosis*, *Science*. 307 (2005) 223–227. <https://doi.org/10.1126/science.1106753>.
- [29] E.F. Queiroz, J.-L. Wolfender, K. Hostettmann, Modern approaches in the search for new lead antiparasitic compounds from higher plants, *Curr. Drug Targets*. 10 (2009) 202–211. <https://doi.org/10.2174/138945009787581113>.
- [30] J.G. Moffat, J. Rudolph, D. Bailey, Phenotypic screening in cancer drug discovery — past, present and future, *Nat. Rev. Drug Discov.* 13 (2014) 588–602. <https://doi.org/10.1038/nrd4366>.
- [31] A.C. Burke, J.S. Dron, R.A. Hegele, M.W. Huff, PCSK9: Regulation and Target for Drug Development for Dyslipidemia, *Annu. Rev. Pharmacol. Toxicol.* 57 (2017) 223–244. <https://doi.org/10.1146/annurev-pharmtox-010716-104944>.

- [32] J. Cameron, T. Ranheim, M.A. Kulseth, T.P. Leren, K.E. Berge, Berberine decreases PCSK9 expression in HepG2 cells, *Atherosclerosis*. 201 (2008) 266–273.
<https://doi.org/10.1016/j.atherosclerosis.2008.02.004>.
- [33] B. Dong, H. Li, A.B. Singh, A. Cao, J. Liu, Inhibition of PCSK9 Transcription by Berberine Involves Down-regulation of Hepatic HNF1 α Protein Expression through the Ubiquitin-Proteasome Degradation Pathway, *J. Biol. Chem.* 290 (2015) 4047–4058.
<https://doi.org/10.1074/jbc.M114.597229>.
- [34] C. Wu, C. Xi, J. Tong, J. Zhao, H. Jiang, J. Wang, Y. Wang, H. Liu, Design, synthesis, and biological evaluation of novel tetrahydroprotoberberine derivatives (THPBs) as proprotein convertase subtilisin/kexin type 9 (PCSK9) modulators for the treatment of hyperlipidemia, *Acta Pharm. Sin. B.* 9 (2019) 1216–1230. <https://doi.org/10.1016/j.apsb.2019.06.006>.
- [35] G.N. Winston-McPherson, H. Xie, K. Yang, X. Li, D. Shu, W. Tang, Discovery of 2,3'-diindolylmethanes as a novel class of PCSK9 modulators, *Bioorg. Med. Chem. Lett.* 29 (2019) 2345–2348. <https://doi.org/10.1016/j.bmcl.2019.06.014>.
- [36] X. Wang, X. Chen, X. Zhang, C. Su, M. Yang, W. He, Y. Du, S. Si, L. Wang, B. Hong, A small-molecule inhibitor of PCSK9 transcription ameliorates atherosclerosis through the modulation of FoxO1/3 and HNF1 α , *EBioMedicine*. 52 (2020) 102650.
<https://doi.org/10.1016/j.ebiom.2020.102650>.
- [37] M.M. Nagiec, J.R. Duvall, A.P. Skepner, E.A. Howe, J. Bastien, E. Comer, J.-C. Marie, S.E. Johnston, J. Negri, M. Eichhorn, J. Vantourout, C. Clish, K. Musunuru, M. Foley, J.R. Perez, M.A.J. Palmer, Novel tricyclic glycal-based TRIB1 inducers that reprogram LDL metabolism in hepatic cells, *MedChemComm*. 9 (2018) 1831–1842. <https://doi.org/10.1039/C8MD00297E>.
- [38] D.N. Petersen, J. Hawkins, W. Ruangsiriluk, K.A. Stevens, B.A. Maguire, T.N. O'Connell, B.N. Rocke, M. Boehm, R.B. Ruggeri, T. Rolph, D. Hepworth, P.M. Loria, P.A. Carpino, A Small-Molecule Anti-secretagogue of PCSK9 Targets the 80S Ribosome to Inhibit PCSK9 Protein Translation, *Cell Chem. Biol.* 23 (2016) 1362–1371.
<https://doi.org/10.1016/j.chembiol.2016.08.016>.
- [39] A.T. Londregan, L. Wei, J. Xiao, N.G. Lintner, D. Petersen, R.G. Dullea, K.F. McClure, M.W. Bolt, J.S. Warmus, S.B. Coffey, C. Limberakis, J. Genovino, B.A. Thuma, K.D. Hesp, G.E. Aspnes, B. Reidich, C.T. Salatto, J.R. Chabot, J.H.D. Cate, S. Liras, D.W. Piotrowski, Small Molecule Proprotein Convertase Subtilisin/Kexin Type 9 (PCSK9) Inhibitors: Hit to Lead

Optimization of Systemic Agents, *J. Med. Chem.* 61 (2018) 5704–5718.

<https://doi.org/10.1021/acs.jmedchem.8b00650>.

- [40] J. Taechalertrpaisarn, B. Zhao, X. Liang, K. Burgess, Small Molecule Inhibitors of the PCSK9-LDLR Interaction, *J. Am. Chem. Soc.* 140 (2018) 3242–3249.
<https://doi.org/10.1021/jacs.7b09360>.
- [41] B.J. Evison, J.T. Palmer, G. Lambert, H. Treutlein, J. Zeng, B. Nativel, K. Chemello, Q. Zhu, J. Wang, Y. Teng, W. Tang, Y. Xu, A.K. Rathi, S. Kumar, A.K. Suchowerska, J. Parmar, I. Dixon, G.E. Kelly, J. Bonnar, A small molecule inhibitor of PCSK9 that antagonizes LDL receptor binding via interaction with a cryptic PCSK9 binding groove, *Bioorg. Med. Chem.* 28 (2020) 115344. <https://doi.org/10.1016/j.bmc.2020.115344>.
- [42] C. Gustafsen, D. Olsen, J. Vilstrup, S. Lund, A. Reinhardt, N. Wellner, T. Larsen, C.B.F. Andersen, K. Weyer, J. Li, P.H. Seeberger, S. Thirup, P. Madsen, S. Glerup, Heparan sulfate proteoglycans present PCSK9 to the LDL receptor, *Nat. Commun.* 8 (2017) 1–14.
<https://doi.org/10.1038/s41467-017-00568-7>.
- [43] W.L. Petrilli, G.C. Adam, R.S. Erdmann, P. Abeywickrema, V. Agnani, X. Ai, J. Baysarowich, N. Byrne, J.P. Caldwell, W. Chang, E. DiNunzio, Z. Feng, R. Ford, S. Ha, Y. Huang, B. Hubbard, J.M. Johnston, M. Kavana, J.-M. Lisnock, R. Liang, J. Lu, Z. Lu, J. Meng, P. Orth, O. Palyha, G. Parthasarathy, S.P. Salowe, S. Sharma, J. Shipman, S.M. Soisson, A.M. Strack, H. Youm, K. Zhao, D.L. Zink, H. Zokian, G.H. Addona, K. Akinsanya, J.R. Tata, Y. Xiong, J.E. Imbriglio, From Screening to Targeted Degradation: Strategies for the Discovery and Optimization of Small Molecule Ligands for PCSK9, *Cell Chem. Biol.* (2019).
<https://doi.org/10.1016/j.chembiol.2019.10.002>.
- [44] T. Aoki, I. Hyohdoh, N. Furuichi, S. Ozawa, F. Watanabe, M. Matsushita, M. Sakaitani, K. Morikami, K. Takanashi, N. Harada, Y. Tomii, K. Shiraki, K. Furumoto, M. Tabo, K. Yoshinari, K. Ori, Y. Aoki, N. Shimma, H. Iikura, Optimizing the Physicochemical Properties of Raf/MEK Inhibitors by Nitrogen Scanning, *ACS Med. Chem. Lett.* 5 (2014) 309–314.
<https://doi.org/10.1021/ml400379x>.
- [45] L.D. Pennington, M.D. Croghan, K.K.C. Sham, A.J. Pickrell, P.E. Harrington, M.J. Frohn, B.A. Lanman, A.B. Reed, M.R. Lee, H. Xu, M. McElvain, Y. Xu, X. Zhang, M. Fiorino, M. Horner, H.G. Morrison, H.A. Arnett, C. Fotsch, A.S. Tasker, M. Wong, V.J. Cee, Quinolinone-based

- agonists of S1P1: Use of a N-scan SAR strategy to optimize in vitro and in vivo activity, *Bioorg. Med. Chem. Lett.* 22 (2012) 527–531. <https://doi.org/10.1016/j.bmcl.2011.10.085>.
- [46] H. Schönherr, T. Cernak, Profound Methyl Effects in Drug Discovery and a Call for New C-H Methylation Reactions, *Angew. Chem. Int. Ed.* 52 (2013) 12256–12267. <https://doi.org/10.1002/anie.201303207>.
- [47] C.S. Leung, S.S.F. Leung, J. Tirado-Rives, W.L. Jorgensen, Methyl Effects on Protein–Ligand Binding, *J. Med. Chem.* 55 (2012) 4489–4500. <https://doi.org/10.1021/jm3003697>.
- [48] B. Belleau, J. Burba, M. Pindell, J. Reiffenstein, Effect of Deuterium Substitution in Sympathomimetic Amines on Adrenergic Responses, *Science*. 133 (1961) 102–104. <https://doi.org/10.1126/science.133.3446.102>.
- [49] A. Mullard, FDA approves first deuterated drug, *Nat. Rev. Drug Discov.* 16 (2017) 305–305. <https://doi.org/10.1038/nrd.2017.89>.
- [50] A. Mullard, Deuterated drugs draw heavier backing, *Nat. Rev. Drug Discov.* 15 (2016) 219–221. <https://doi.org/10.1038/nrd.2016.63>.
- [51] G.S. Timmins, Deuterated drugs: where are we now?, *Expert Opin. Ther. Pat.* 24 (2014) 1067–1075. <https://doi.org/10.1517/13543776.2014.943184>.
- [52] T.G. Gant, Using Deuterium in Drug Discovery: Leaving the Label in the Drug, *J. Med. Chem.* 57 (2014) 3595–3611. <https://doi.org/10.1021/jm4007998>.
- [53] T. Pirali, M. Serafini, S. Cargnin, A.A. Genazzani, Applications of Deuterium in Medicinal Chemistry, *J. Med. Chem.* 62 (2019) 5276–5297. <https://doi.org/10.1021/acs.jmedchem.8b01808>.
- [54] K. Müller, C. Faeh, F. Diederich, Fluorine in Pharmaceuticals: Looking Beyond Intuition, *Science*. 317 (2007) 1881–1886. <https://doi.org/10.1126/science.1131943>.
- [55] S. Purser, P.R. Moore, S. Swallow, V. Gouverneur, Fluorine in medicinal chemistry, *Chem. Soc. Rev.* 37 (2008) 320–330. <https://doi.org/10.1039/B610213C>.
- [56] J. Wang, M. Sánchez-Roselló, J.L. Aceña, C. del Pozo, A.E. Sorochinsky, S. Fustero, V.A. Soloshonok, H. Liu, Fluorine in Pharmaceutical Industry: Fluorine-Containing Drugs Introduced to the Market in the Last Decade (2001–2011), *Chem. Rev.* 114 (2014) 2432–2506. <https://doi.org/10.1021/cr4002879>.
- [57] B.K. Park, N.R. Kitteringham, P.M. O'Neill, Metabolism of Fluorine-Containing Drugs, *Annu. Rev. Pharmacol. Toxicol.* 41 (2001) 443–470. <https://doi.org/10.1146/annurev.pharmtox.41.1.443>.

- [58] P. Shah, A.D. Westwell, The role of fluorine in medicinal chemistry, *J. Enzyme Inhib. Med. Chem.* 22 (2007) 527–540. <https://doi.org/10.1080/14756360701425014>.
- [59] W.K. Hagmann, The Many Roles for Fluorine in Medicinal Chemistry, *J. Med. Chem.* 51 (2008) 4359–4369. <https://doi.org/10.1021/jm800219f>.
- [60] D. O'Hagan, Fluorine in health care: Organofluorine containing blockbuster drugs, *J. Fluor. Chem.* 131 (2010) 1071–1081. <https://doi.org/10.1016/j.jfluchem.2010.03.003>.
- [61] E.P. Gillis, K.J. Eastman, M.D. Hill, D.J. Donnelly, N.A. Meanwell, Applications of Fluorine in Medicinal Chemistry, *J. Med. Chem.* 58 (2015) 8315–8359. <https://doi.org/10.1021/acs.jmedchem.5b00258>.
- [62] J.A. Olsen, D.W. Banner, P. Seiler, U.O. Sander, A. D'Arcy, M. Stihle, K. Müller, F. Diederich, A Fluorine Scan of Thrombin Inhibitors to Map the Fluorophilicity/Fluorophobicity of an Enzyme Active Site: Evidence for C-F \cdots C=O Interactions, *Angew. Chem.* 115 (2003) 2611–2615. <https://doi.org/10.1002/ange.200351268>.
- [63] I. Hyohdoh, N. Furuichi, T. Aoki, Y. Itezono, H. Shirai, S. Ozawa, F. Watanabe, M. Matsushita, M. Sakaitani, P.-S. Ho, K. Takanashi, N. Harada, Y. Tomii, K. Yoshinari, K. Ori, M. Tabo, Y. Aoki, N. Shimma, H. Iikura, Fluorine Scanning by Nonselective Fluorination: Enhancing Raf/MEK Inhibition while Keeping Physicochemical Properties, *ACS Med. Chem. Lett.* 4 (2013) 1059–1063. <https://doi.org/10.1021/ml4002419>.
- [64] P.M. Giles, B.J. Andrews, J. Cheshire, N. Noble, D.P.R. Muller, J. Slack, O.H. Wolff, Effects of delipidated serum and lipoprotein-deficient serum on sterol biosynthesis and efflux in cultured skin fibroblasts—a comparison of the behaviour of cells from a control with those from a heterozygote and homozygote for familial hypercholesterolaemia, *Clin. Chim. Acta.* 113 (1981) 183–191. [https://doi.org/10.1016/0009-8981\(81\)90152-2](https://doi.org/10.1016/0009-8981(81)90152-2).
- [65] E. Scotti, C. Hong, Y. Yoshinaga, Y. Tu, Y. Hu, N. Zelcer, R. Boyadjian, P.J. de Jong, S.G. Young, L.G. Fong, P. Tontonoz, Targeted Disruption of the Idol Gene Alters Cellular Regulation of the Low-Density Lipoprotein Receptor by Sterols and Liver X Receptor Agonists, *Mol. Cell. Biol.* 31 (2011) 1885–1893. <https://doi.org/10.1128/MCB.01469-10>.
- [66] I. González, J. Mosquera, C. Guerrero, R. Rodríguez, J. Cruces, Selective Monomethylation of Anilines by Cu(OAc)₂-Promoted Cross-Coupling with MeB(OH)₂, *Org. Lett.* 11 (2009) 1677–1680. <https://doi.org/10.1021/ol802882k>.

Declaration of interests

The authors declare that they have no known competing financial interests or personal relationships that could have appeared to influence the work reported in this paper.

The authors declare the following financial interests/personal relationships which may be considered as potential competing interests:

Patent applications containing compounds in this manuscript have been filed.